FMCW RADAR ALTIMETER TEST BOARD

A THESIS SUBMITTED TO
THE GRADUATE SCHOOL OF NATURAL AND APPLIED SCIENCES
OF
THE MIDDLE EAST TECHNICAL UNIVERSITY

BY

AYDIN VURAL

IN PARTIAL FULFILLMENT OF THE REQUIREMENTS FOR THE DEGREE OF
MASTER OF SCIENCE
IN
THE DEPARTMENT OF ELECTRICAL AND ELECTRONICS ENGINEERING

DECEMBER 2003

Approval of the Graduate School of Natural and Applied Sciences

_____

Prof. Dr. Canan ÖZGEN
Director

I certify this thesis satisfies all the requirements as a thesis for the degree of Master of Science.

_____

Prof. Dr. Mübeccel DEMİREKLER
Head of Department

This is to certify that we have read this thesis and that in our opinion it is fully adequate, in scope and quality, as a thesis for the degree of Master of Science.

_____

Prof. Dr. Altunkan HIZAL
Supervisor

Examining Committee Members

Prof. Dr. Nevzat YILDIRIM(Chairman) _____

Prof. Dr. Altunkan HIZAL _____

Prof. Dr. Canan TOKER _____

Assis. Prof. Şimşek DEMİR _____

Dr. Ufuk KAZAK _____

ABSTRACT

FMCW RADAR ALTIMETER TEST BOARD

Vural, Aydın

M.S., Department of Electrical and Electronics Engineering

Supervisor: Prof. Dr. Altunkan Hızal

December 2003, 82 pages

In this thesis, principles of a pulse modulated frequency modulated continuous wave radar is analyzed and adding time delay to transmitted signal in the laboratory environment performed. The transmitted signal from the radar has a time delay for traveling the distance between radar and target. The distance from radar to target is more than one kilometers thus test of the functionality of the radar in the laboratory environment is unavailable.

The delay is simulated regarding to elapsed time for the transmitted signal to be received. This delay achieved by using surface acoustic wave (SAW) delay line in the laboratory environment. The analyses of the components of the radar and the delay line test board are conducted.

Keywords: Radar, FMCW, SAW Delay Line

ÖZ

FMCW RADARLI YÜKSEKLİKÖLÇER TEST KARTI

Vural, Aydın

Yüksek Lisans, Elektrik-Elektronik Mühendisliği

Tez yöneticisi: Prof.Dr. Altunkan HIZAL

Aralık 2003, 82 sayfa

Bu tezde darbe modülasyonlu frekans modülasyonlu sürekli dalga radarı analiz edilmiş ve gönderilen sinyale laboratuar ortamında zaman gecikmesi eklenmesi uygulanmıştır. Radardan gönderilen sinyalde radar ile hedef arasındaki yolculuğundan kaynaklanan bir zaman gecikmesi vardır. Radar ile hedef arasındaki mesafe bir kilometreden fazla olduğu için radarın fonksiyonel testlerini laboratuar ortamında yapmak mümkün değildir.

Gönderilen sinyalin geri alınması sırasında geçen zamana bağlı olarak gecikme simülasyonu yapılmıştır. Bu gecikme yüzey akustik dalga gecikme hattı kullanılarak laboratuar ortamında elde edilmiştir. Radar elemanlarının ve gecikme hattı test kartının analizleri yapılmıştır.

Anahtar Kelimeler: Radar, FMCW, SAW Gecikme hattı

TABLE OF CONTENTS

LIST OF TABLES

LIST OF FIGURES

CHAPTER 1

RADAR

1.1 Introduction

Radar is an electromagnetic system for the detection and location of objects. Radar transmits a form of electromagnetic energy such as pulsed modulated wave and receives the reflected electromagnetic energy back from the object. The basic radar consists of a transmitter antenna which transmits the energy from a kind of oscillator and a receiving antenna which receives the reradiated energy from the object in the path of radiation and a receiver [1]. The receiving antenna collects the reflected energy and delivers it to the receiver for determining necessary information such as presence, range, location and relative velocity of the target. The range is determined calculating how long the round trip transmission-reflection took. The relative velocity is calculated from Doppler Effect (the frequency shift of the transmitted energy when it received back) and location is determined by measuring the direction of receiving wavefront. If your waves are focused in a narrow beam, you can know the direction of the object by moving the beam from side to side. The radar's antenna, in many cases a parabolic metal dish, takes the energy from the transmitter, directs it in a narrow beam towards the target, and then receives echoes reflected back from the target. Other radar antennas have beams that are moved electronically. These "phased array" radars are mostly used for military applications. Since radio waves travel just as easily in the

dark as in the daytime, radar is a way of seeing things in the dark, and through clouds and fog.

1.2 Radar Development

Today RADAR is a common word in vocabularies but it derived from the expression ***ra****dio* ***d****etection* ***a****nd* ***r****anging*. The basic concepts of radar were developed in the late 19th and early 20th centuries. The actual development of radar is between World War I and World War II as a tool for detecting enemy aircrafts from long distances. However, it was just before and during World War II that radar emerged as a practical engineering device. Hülsmeyer, a German engineer experimented the first detection of reflected electromagnetic energy from a ship in 1903. But because of the inadequate technology the range of detection was a little more than about a mile. Detecting enemy planes and ships and of navigating across land and sea with the aid of invisible radio waves attracted the attention of military researchers. In the 1930s, several laboratories developed early versions of radar systems such as U.S. Naval Research Laboratory (NRL). In the United States, radar was born and developed at the NRL in the mid-1930s. The first detection of an aircraft is in 1930 by L. A. Hayland from NRL. The operating frequency of this radar was around 26 MHz. By the developing technology the operating frequency of the equipment used in radar systems are increased and higher frequencies used in radars. A list of radar frequencies are given in Appendix A.

Prior to World War II, NRL engineers overcame many obstacles and made great advances in developing radar. These included generating high-pulse power suitable for radar usage; creation of the duplexer, which enabled the transmitter and receiver to be used with a single antenna; development of a suitable map-like display for recognizing

and interpreting information provided by the radar. In the United States much of radar research also took place at the Massachusetts Institute of Technology's (MIT) Radiation Laboratory. Engineers and scientists at Radiation Laboratory designed almost half of the radar deployed in World War II. The radar project in MIT became one of the largest wartime projects ever, employing nearly 4000 people World War II [2]. During the war more than 100 different radar systems were developed there. During World War II radar was used by both the English and the Germans. But it was the perfection of the technology by the England, with further design, development and production support from Canada and the United States, that helped Britain successfully defend itself from Germans. England was very vulnerable to attacks from the German air force, and so in the late 1930s a network of radars was constructed along the southern English coast called "Chain Home". These radars used shortwave pulses to detect incoming German aircrafts for early warning of air attacks.

By the development of radar, its application areas become larger as well. The major use of radar is in military applications such as surveillance, navigation and control and guidance of weapons. Since its use in World War II, radar has been used extensively by the military for a wide variety of missions, such as detection and tracking of aircraft, missiles and satellites, or other space objects. Because of its ability to detect airborne or space borne objects at great ranges (hundreds to thousands of miles), radar is an integral part of most air and missile defense systems. In addition to their current use in military operations, radars have many civilian uses as well. They are used extensively for air traffic control, geographic mapping, aircraft navigation and remote sensing. Radars are

generally capable of performing many tasks but are often categorized according to the main function performed by the system. Some of the common radar types are given below:

Simple Pulse Radar,

Pulse Doppler Radar,

Continuous-Wave (CW) Radar,

Frequency-Modulated Continuous-Wave (FM-CW) Radar,

Moving Target Indication (MTI) Radar,

High-Range-Resolution Radar,

Pulse-Compression Radar,

Synthetic Aperture Radar (SAR),

Inverse Synthetic Aperture Radar (ISAR),

Side-Looking Airborne Radar (SLAR),

Imaging Radar,

Interferometric SAR (IFSAR),

Tracking Radar,

Scatterometer Radar,

Track-While-Scan Radar, and

Electronically Scanned Phased-Array Radar.

In Chapter 2, some fundamental formulations used for radar analysis are given and some of the radar types including Simple Pulse Radar, Continuous Wave (CW) Radar, Frequency Modulated Continuous Wave (FMCW) Radar and Pulse Frequency Modulated CW Radar are mentioned briefly.

CHAPTER 2

ELECTROMAGNETIC FUNDEMENTALS OF RADAR

2.1 Basic Radar Systems

Radar operating principle is based upon the scattering properties of electromagnetic waves which reflect from various objects. In a radar system the electromagnetic wave travels in various media and scatters from any object. The incident wave scatters from the object and the receiver of the radar system detects the reflected wave from the object (target). Figure (2.1) is the simplified scheme of a monostatic radar system [3].

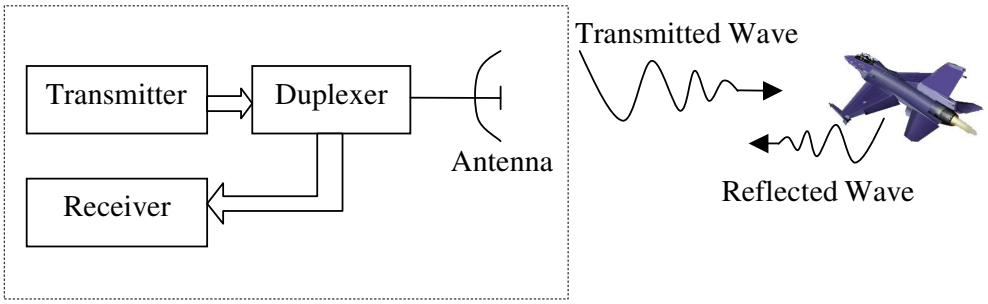

Figure 2.1 Monostatic radar system

Monostatic radar utilizes a common antenna both for transmitting and receiving. Monostatic radars are more conventional compared to bistatic radars. A bistatic radar is one in which the transmitting and receiving antenna separated by a considerable distance. Figure (2.2) is the simplified scheme of a basic bistatic radar system.

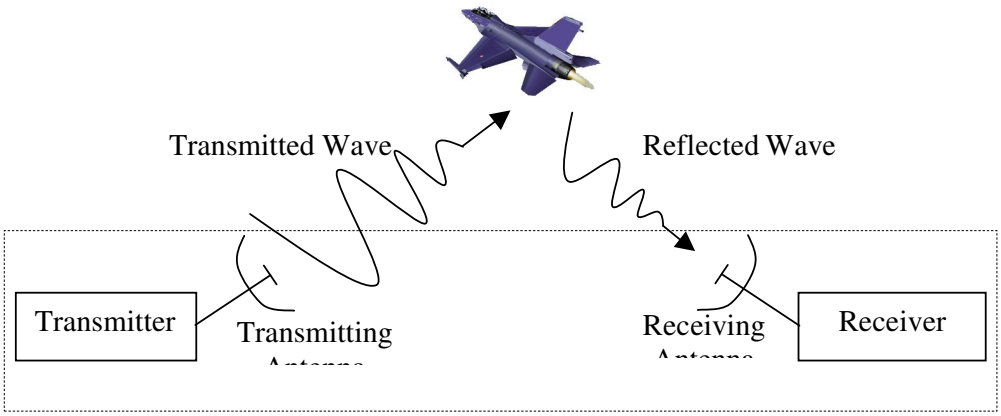

Figure 2.2 Bistatic radar system

The radar measurements for the bistatic radars are much more complicated and difficult to accomplish when compared to conventional monostatic radars.

2.2 Radar Equation

The most important aspect of radar is the radar equation. Radar equation includes all relation between the transmitted and reflected power. The most general case of the radar range equation is for the bistatic radar range equation, that is:

$$P_r = P_t \frac{G_t}{4 \pi R_t^2} \frac{\sigma}{4 \pi R_r^2} \frac{G_r \lambda^2}{4\pi} \qquad (2.2)$$

where;

P_r = reflected power at the receiver antenna site,

P_t = transmitted power from the transmitter antenna,

G_t = gain of the transmitting antenna,

G_r = gain of the receiving antenna,

σ = radar cross section,

λ = wavelength of the signal,

R_t = distance from target to transmitting antenna,

R_r = distance from target to receiving antenna.

Equation (2.2) does not include polarization and reflection losses. We can divide the radar range equation into smaller pieces so that we can understand the whole equation. Power flux density incident on the target is

$$P_t \frac{G_t}{4 \pi R_t^2} \tag{2.3}$$

Gain of the antenna (G) is defined as the ratio of the intensity, in given direction, to the radiation intensity that would be obtained if the power accepted by the antenna were radiated isotropically. Another sub equation;

$$\frac{\sigma}{4\pi R_r^2} \tag{2.4}$$

defines the isotropically scattered power density at the position of the receiving antenna. Radar cross section of the target is σ. The final part of the equation

$$\frac{G_r \lambda^2}{4\pi} \tag{2.5}$$

defines the effective area of the receiving antenna. Effective area represents the amount of the physical area of an antenna that serves as an electrical antenna.

Radar range equation constructs the fundamentals of the radar system principles. Equation (2.1) has given for a bistatic radar system (Figure 2.1) which the transmitting and receiving antennas are located at different locations. For monostatic radar systems (Figure 2.2) which one antenna is used for both transmitting and receiving purposes, the radar range equation can be written as

$$P_r = P_t \frac{G}{4 \pi R^2} \frac{\sigma}{4 \pi R^2} \frac{G \lambda^2}{4\pi} = \frac{P_t G^2 \lambda^2 \sigma}{(4\pi)^3 R^4} \tag{2.6}$$

where R_t and R_r is equal to each other and represented by R. Receiving and transmitting antennas are the same so the distance from receiving antenna to target (R_r) is equal to transmitting antenna to target (R_t). Equation (2.6) expresses the power received from a target at distance R and whose RCS is σ, the operating wavelength is λ and the gain of the antenna is G. In this simple form of radar equation losses that occurs from the radar system are not included. In actual radar systems some of these losses are very real and cannot be ignored.

2.3 Radar Cross Section

In radar terminology another important property of the targets is the radar cross section, i.e. σ in Equation (2.4). Radar cross section (σ) or RCS of a target is defined by as the area intercepting that amount of power which, when scattered isotropically, produces at the receiver a density which is equal to that scattered by the actual target [4].

RCS is

Table 2.1 RCSs of some objects at microwave frequencies

Object	Typical RCS
Pickup Truck	200
Automobile	100
Large bomber or jet airliner	40
Medium bomber	20
Large fighter aircraft	6
Small fighter aircraft	2
Human being	1
Conventional winged missile	0,5
Bird	0,01

used to determine the scattering characteristics of a target. RCS of a target depends on the shape, size, material, properties of the target and the frequency, polarization and angle of arrival of the incident wave. The unit of RCS of a three dimensional target is square meters. Table (2.1) gives RCSs of some objects.

2.4 Common Types of Radar

2.4.1 Pulse Radar

Pulse radar is the common radar type used today. The transmitted waveform is a train of narrow rectangular pulses modulating a sinewave carrier. The transmitter is turned on and off to generate repetitive train of pulses. Peak power and duration of the pulses and pulse repetitions frequency (prf) changes regarding to functionality of the radar. After a pulse is transmitted, radar listens for the echoes from the targets until the next pulse transmitted. The distance of the target is determined by the amount of time transmitted signal is traveled from antenna to object of interest (target) and back from object to the antenna.

Since electromagnetic energy propagates at the speed of light c = 2.99795 x 10^{8} m/s, the range R is

$$R = \frac{cT_R}{2} \tag{2.7}$$

T_R is the total time elapsed between the transmission of the wave and receiving the reflected wave from the target. In Equation (2.7) division by 2 comes from the two way propagation of the wave. Figure (2.3) show a simplified diagram of a pulse radar system.

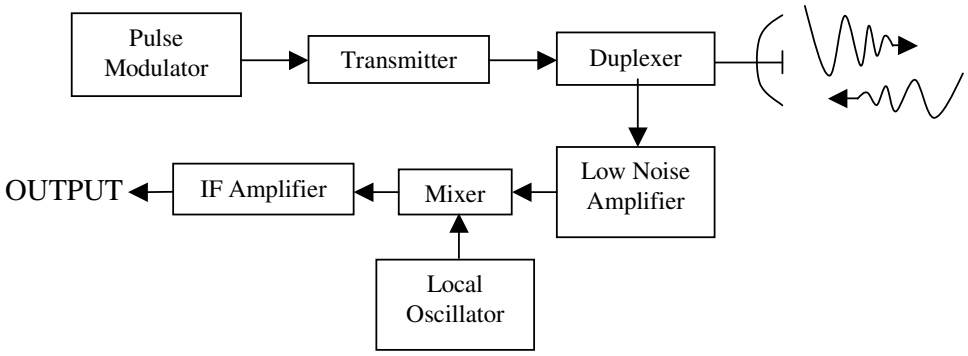

Figure 2.3 Pulse radar system

When the distance of the target is so long the reflected wave can be received after the second pulse transmitted so ambiguities may occur. The maximum unambiguous distance is related to pulse repetition frequency (f_p) and given by equation (2.8). Higher pulse repetition interval results longer unambiguous distance. Range ambiguities can be avoided by lowering the pulse repetition frequency and this means a low sampling rate.

Equation (2.8) is applicable for monostatic pulse radars which have a common antenna used for transmitting and receiving the signal.

$$R_{unamb} = \frac{c}{2f_p} \tag{2.8}$$

The very first application of range determination by pulsed signals was in 1925 by Breit and Tuve for measuring the height of ionosphere [5].

The maximum distance R_{max} of the pulsed radar is directly proportional to pulse repetition interval. Increasing the pulse repetition interval will increase the

maximum distance of the radar system. Pulse repetition period is determined essentially by the distance of the expected targets.

$$R_{\max} = \frac{cT_p}{2} \tag{2.9}$$

A pulse radar that extracts the doppler frequency shift for the detection of the moving targets it's called a pulse doppler radar.

2.4.2 Continuous Wave (CW) Radar

Continuous wave radars transmit a signal which oscillates with a frequency of f_0. Some of the transmitted signal reflects from the existing target and reflected signal collected by the receiving antenna. If the target is in motion relative to the radar a doppler shift in the frequency of the received signal will occur. If this is the case the frequency of the received signal will be $f_0 \pm f_d$. If the distance from target to radar is decreasing (a closing target) the oscillation frequency f_0 will increase by f_d, otherwise if the distance is increasing (a receding target) the oscillation frequency will decrease by f_d. A simplified diagram of the continuous wave radar is given in Figure (2.4).

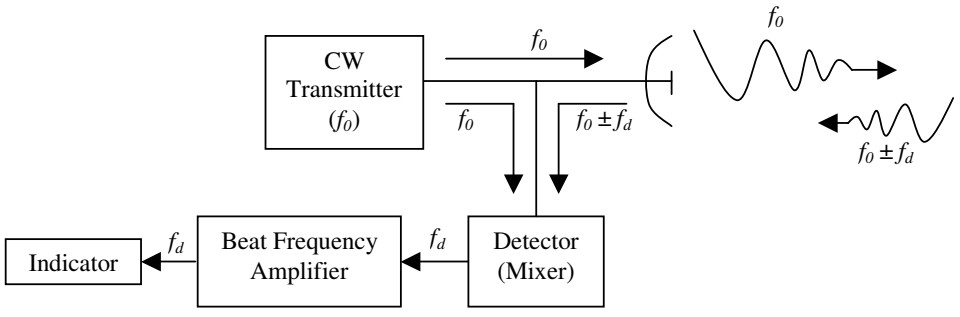

Figure 2.4 CW radar system

This type of radar is commonly used for traffic regulation. The speed indicator used by the policemen is a kind of CW radar. The frequency shift f_d is proportional to oscillation frequency f_0 and the relative velocity of the target v_r.

$$v_r = \frac{f_d \times c}{2f_0} \tag{2.10}$$

The graph of Doppler frequency as a function of oscillation frequency and some relative target velocities calculated using MATLAB 6.5 is given in Appendix B. An interesting example of the CW radar is the proximity fuze widely used during World War II. This fuze is one of the first examples of the proximity fuzes which operate by the principles of radar.

2.4.3 Frequency Modulated Continuous Wave (FMCW) Radar

Frequency Modulated Continuous Wave (FMCW) radar is a kind of continuous wave radar. Continuous wave radars are unable to measure the distance between radar and target. To measure the distance a sort of timing signal must be applied to the continuous wave carrier. In the FMCW radar the timing mark can be achieved by frequency modulating the continuous wave carrier. The changing frequency acts as a time marker and the elapsed time between transmission and the receiving the reflected wave can be calculated from the difference in frequency of the reflected signal and the transmitter. Another advantage of the FMCW radar system is simplicity of design when compared to a pulsed radar system. Block diagram of a typical FMCW radar system may be seen in Figure (2.5).

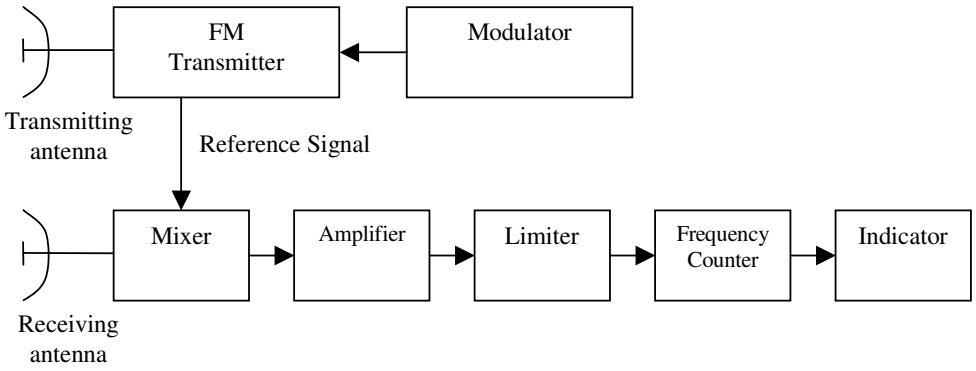

Figure 2.5 FMCW radar system

In FMCW radar systems the common frequency source is a voltage controlled oscillator (VCO). The modulation frequency cannot increase continually and must be periodic, thus VCO is usually controlled by a sawtooth wave shape generator. When the VCO is controlled by sawtooth wave shape generator the characteristics of the modulated signal may be seen in Figure (2.6). In Figure (2.6);

$f_m = 1 / T_m$ = Modulation frequency,

$f_{max} - f_{min} = \Delta f$ = Frequency deviation,

T_d = Delay time.

The frequency difference between the transmitted signal and the received signal indicates the distance between radar and the target. This frequency is the major identifier for distance measurement and called the *beat frequency* (f_b). The beat frequency f_b, is the indicator of the distance between radar and target. For amplitude fluctuations the beat frequency is amplified by a low frequency amplifier and then limited by a limiter. The distance R can be calculated from Equation (2.11).

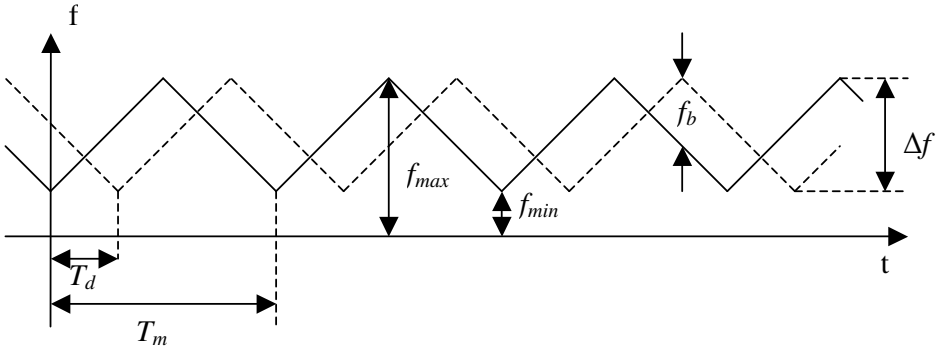

Figure 2.6 Frequency variation of transmitted and received signal

In Equation (2.11), f_m is the modulation frequency and c is the speed of light where Δf is the deviation of the modulation frequency which is the difference between the maximum and the minimum frequency of the transmitted signal.

$$R = \frac{f_b \; c}{4 f_m \; \Delta f} \tag{2.11}$$

The greater the deviation of the transmitted signal in a given time interval, the more accurate the transit time (T_d) can be measured and this result a greater transmitted spectrum. Speed of light, modulation frequency (f_m) and the deviation of the modulation frequency (Δf) is assumed to be constant, thus the distance from radar to the target is a function of the beat frequency (f_b). For some different values of frequency deviation and modulation frequency, beat frequency versus distance from radar to target is given in Figure (2.7) and Figure (2.8).

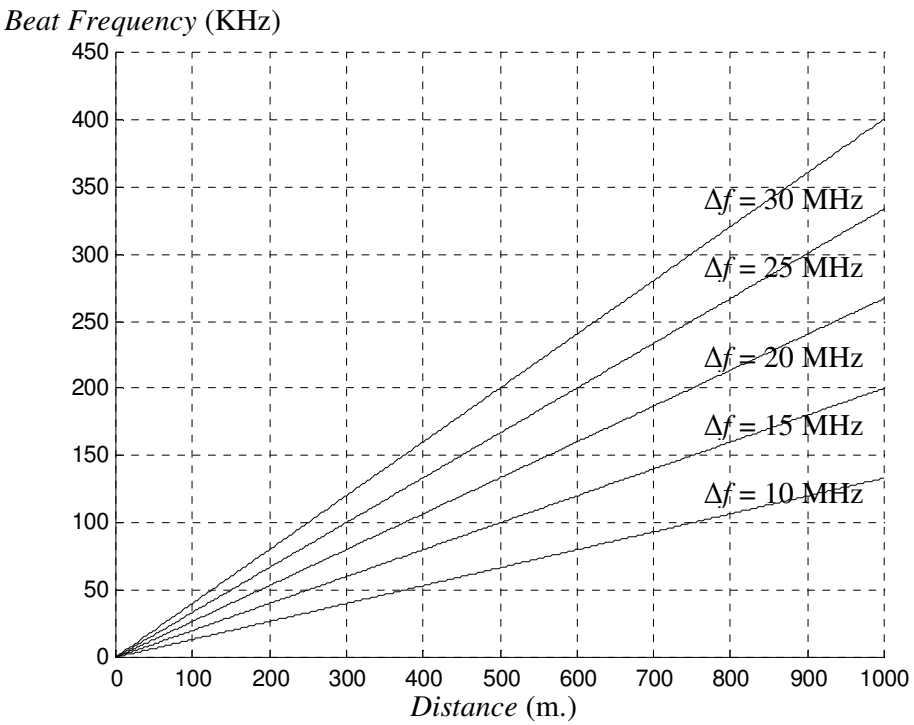

Figure 2.7 Beat frequency variation (f_m = 1 KHz)

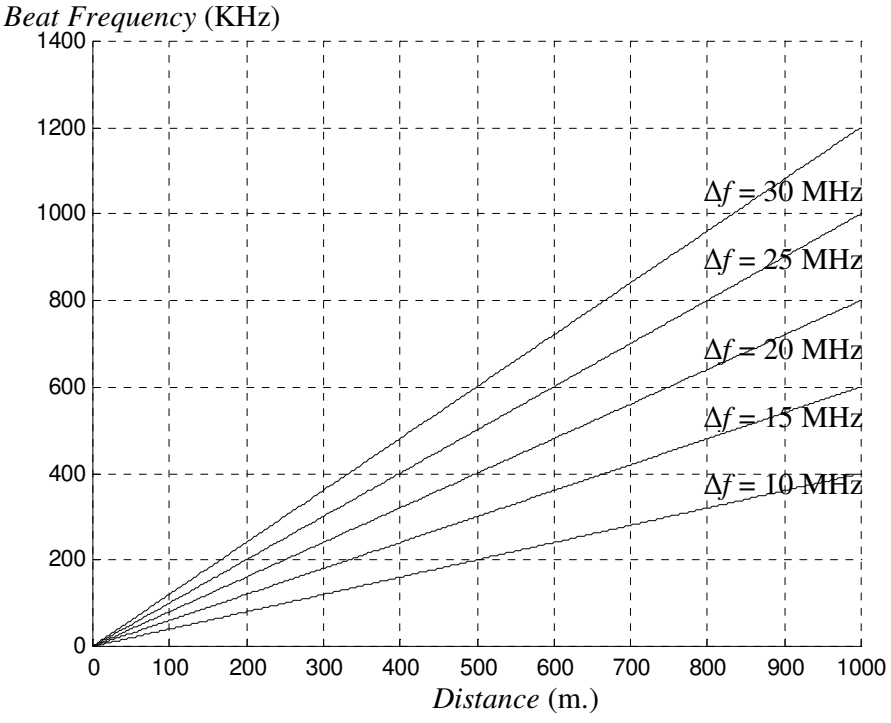

Figure 2.8 Beat frequency variation (f_m = 3 KHz)

The choice of frequency modulation and modulation deviation is determined by the ranging sensitivity, K = $4f_m\Delta f$ / c (Hz/m). For example if a VCO is linearly modulated at a rate of 10 KHz per over a range of 1 GHz the beat frequency of the FMCW system will be 133 KHz per meter of range. A wider range of frequencies swept by the modulation waveform and a higher frequency of the modulating waveform will yield more accurate measurement of the range information. Another consideration for beat frequency and doppler shift must be made if the radar or the target is in motion. A frequency shift by doppler effect will be superimposed on the beat note and an erroneous range measurement results. The doppler frequency shift will causes the beat frequency echo signal to be shifted up or down by doppler shift (f_d). Figure (2.9) illustrates the beat frequency time plot of the echo signal. On the time plot of the beat frequency the doppler shift can be seen in Figure (2.10).

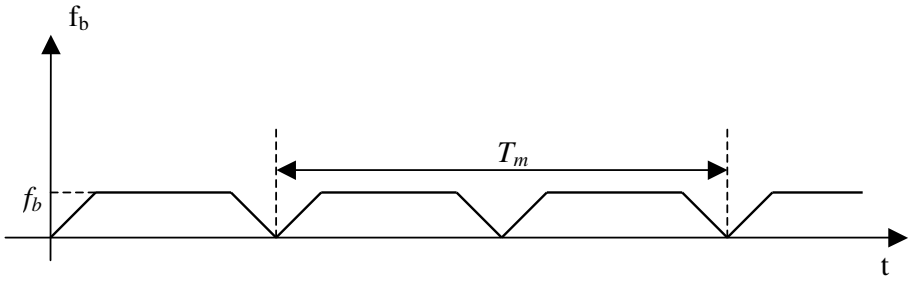

Figure 2.9 Beat frequency variation in time (for stationary objects)

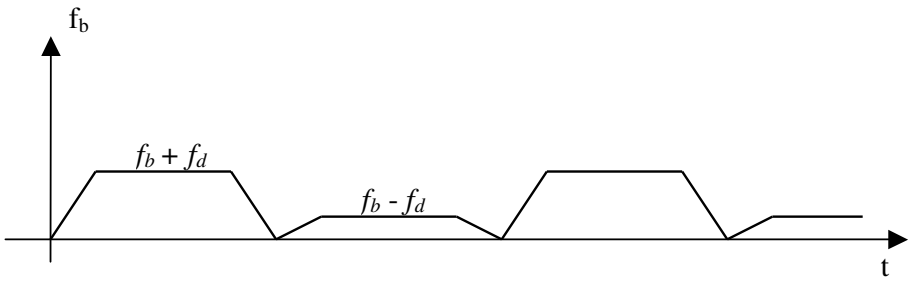

Figure 2.10 Beat frequency variation in time (for moving objects)

The doppler shift resulting from the moving platforms will yield smaller doppler shift compared to beat frequency. Assume that the FMCW radar frequency is around 850 MHz with modulation frequency (f_m) is 3 KHz and modulation deviation (Δf) is 30 MHz. The beat frequency for a target at a distance of 1000 meters is

$$f_b = \frac{4 f_m \Delta f R}{c} = \frac{4 \times 3 \times 3 \times 10^{13}}{3 \times 10^8} \text{ Hz} = 1200 \text{ kHz}$$

and if the target is moving towards the radar with a radial velocity of 500 km/h (139 m/s) the doppler shift of the received frequency is only

$$f_b = \frac{2 f_0 v}{c} = \frac{2 \times 850 \times 10^6 \times 139}{3 \times 10^8} = 787.67 \text{ Hz}$$

The frequency shift due to doppler effect is only 787.67 Hz whilst the beat frequency is 1.2 MHz. When designing FMCW radar this doppler shift in this example can be neglected regarding to the application area and the design frequencies of the radar. If the target is in motion and the beat signal contains a component due to doppler frequency shift, the range frequency (f_b–f_d) can be extracted from the received signal. The achieve the range frequency, average of the beat signal frequency is measured and the modulation waveform

must have equal upsweep and downsweep regarding the doppler frequency shift. Also when the average of the beat frequency is measured for one cycle of the modulation frequency, the doppler effect will be cancelled.

2.4.4 Pulse Modulated FMCW Radar

Another type of the FMCW radar is the pulse modulated FMCW radar. In the pulse modulated FMCW radar, the transmitter transmits the signal only for a limited time interval and then the receiver listen for the echoes of the transmitted signal.

In pulse modulated FMCW radar the transmitted signal reflects back from the target and the frequency of the received signal compared with the modulator frequency. Beat frequency is the difference between the modulator frequency and the received signal. The modulator frequency acts as a time marker as in the FMCW radar. Except from the FMCW radar the pulse modulated radar has blind range. Blind range occurs when the signal pulse is transmitted because the receiver is blocked within the time period of transmission.

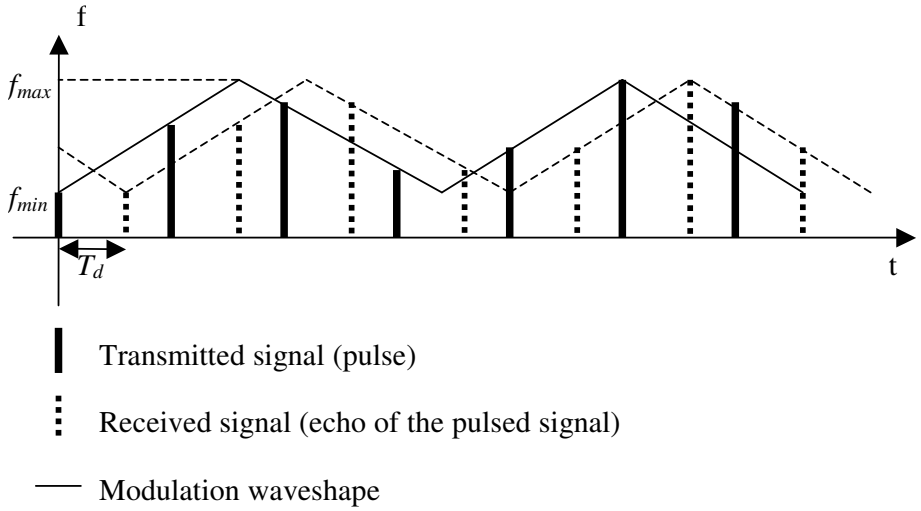

Figure 2.11 Pulse modulated FMCW radar frequency variation

Despite the range limitation of the pulse radar that is limited to a value depending on the unambiguous distance (R_{unamb}) given in Equation (2.8), the pulse modulated FMCW does not have range ambiguities depending on the pulse repetition frequency. Because pulse modulated FMCW radar utilizes the beat frequency measurement instead of time delay measurement. The blind range (R_p) is calculated from Equation (2.12) and the multiples of the blind range are also blind. T_p is the pulse interval.

$$R_p = \frac{cT_p}{2} \tag{2.12}$$

The blind range width is dependant to the pulse width of the transmitted pulse. It is advantageous to reduce the pulse width as short as possible to achieve the minimal blind range width. Actually, FMCW radar also has range ambiguities and maximum range depending to the modulation frequency. The maximum range (R_{max}) is equal to the distance traveled by a wave (velocity = speed of light) within the half period of the frequency modulation. For example, if the modulation frequency is 1 KHz then the maximum unambiguous distance is $T_m/2$ times the speed of light. If this is the case maximum unambiguous distance is 149.897 kilometers. If the distance exceeds the maximum distance ($2R_{max}>R>R_{max}$) the calculated beat frequency peak will be

$$f_b = \frac{4 \times f_m \times \Delta f \times \left(2 \times R_{max} - R\right)}{c} \tag{2.13}$$

Equation (2.13) results from the downsweeping of the triangular waveform. When the distance (R) is longer from the maximum distance (R_{max}) the modulation frequency slope changes its sign from positive to negative or vice versa after the delay time (t_d) corresponding to distance of the

target. This theoretical result does not occur because the maximum distance is usually much longer from the target distance at the FMCW radar applications. If the modulation frequency f_m is equal to 3 KHz, the maximum distance R_{max} will be 100 kilometers. And if the target distance is longer than 100 km then we can easily change the modulation frequency to a higher value then 3 KHz and these situations are usually well defined at the design phase.

CHAPTER 3

SURFACE ACOUSTIC WAVE (SAW) DEVICES

3.1 Introduction to SAW Devices

Integrated Circuits (IC) are small and contain many elements up to 10^8. At the same time it is important that ICs contain only transistors, diodes, resistors and capacitors. Practically inductive elements cannot be integrated in monolithic ICs.

With the development of ICs, the problem of miniaturization of filters, delay lines and other components that included inductive elements appeared. As a result of search of ways to miniaturize mentioned components, surface acoustic wave (SAW) devices were created.

The fundamentals of this technique lie in the discovery of the piezoelectricity by the brother Curie in 1880 and of the surface acoustic waves in 1885 which is the basis of the SAW devices by the famous English scientist Lord Rayleigh. Piezoelectricity is a coupling between elastic deformation and electric polarization which exists in certain crystals such as quartz. Surface waves are piezoelectric microwaves which can be propagated over the surface of these crystals at a velocity of the order 3500 m/s. After the studies of Rayleigh, the surface acoustic waves are first observed at the beginning of the twentieth century that an earthquake could be detected at a great distance by two tremors corresponding to the modes of volume propagation, transverse and longitudinal modes and one tremor corresponds to surface propagation on the earth's

crust in the form of acoustic waves which arrived later from the first two modes.

The application of SAW begins from 1965 with the invention of an effective piezoelectric transducer, in the form of an Interdigital Comb, by White and Walter [6]. This transducer implemented on a substrate by photolithographic methods using the means of microelectronic techniques. Acoustic surface waves nowadays called Rayleigh waves are useful because the propagation of these waves is very much smaller compared to the velocity of the electromagnetic waves. So the associated components with the surface acoustic waves are smaller too. The very first application of the SAW devices is in the area of military which uses pulse compression in modern radar and sonar in 1965–1970. Today SAW devices have many applications, every modern television have at least one receiver with a SAW filter and many of the telecommunication system, satellite systems, and smaller radar systems utilizes the high performance SAW filter techniques. The nonlinear properties of the SAW materials form the basis of the frequency multiplication and the systems uses oscillator with the low frequency quartz crystal followed by a frequency multiplier chain replaced with high frequency SAW precise oscillators.

The SAW devices have may advantages such as low marginal cost, excellent reproducibility, electrical and mechanical robustness. The large frequency range of these devices and the flexibility of the SAW oscillator by adapting the peak voltage to the desired function to utilize an oscillator tunable over a wide frequency range, a frequency modulated oscillator or a very stable frequency generator, adds another advantage to these devices. And the interaction of the acoustic wave with an external wave such as a light wave, a wave in the space charge associated with

the movements of electrons or a magnetic wave results the large application area of the SAW devices.

3.2 Theory of SAW Devices

The design goal of the filter is to select material for the waveguide, determine the main filter dimensions, and examine its frequency characteristics correspondence to the given specification.

The main electrical parameters (central frequency of the pass-band f_0 and bandwidth ΔF of the filter) are presented as initial data for design calculations.

The goal of the calculations is to select material for the waveguide, determine main dimensions of filter elements and examine its frequency characteristics correspondence to the given specification.

Interdigital Transducers (IDTs) are the main elements of a SAW filter consisting of input transducer, waveguide and output transducer. An IDT is shown in Figure (3.1). Most of the SAW devices use materials like quartz, lithium niobate ($LiNbO_3$) and lithium tantalite ($LiTaO_3$). Strong electromechanical coupling factors (k^2) makes these crystals preferable but these crystals are very temperature sensitive so they are excluded from certain functions. The double oxide of bismuth and germanium ($Bi_{12}GeO_{20}$) has a SAW velocity which is approximately half of the SAW velocities of the other crystals given in Table (3.1). For the realization of long delay lines with $Bi_{12}GeO_{20}$ will be preferable compared to some other crystals. Gallium arsenide (GaAs) has a double advantage of being piezoelectric and semiconducting. By the piezoelectric and the semiconducting properties of the gallium arsenide the realization of integrated acoustic and microelectronic device both on the same substrate allowed.

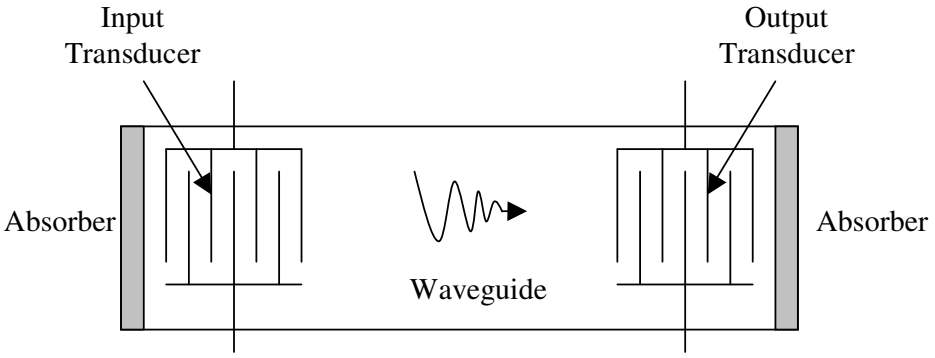

Figure 3.1 SAW filter

Table 3.1 Parameters of piezoelectric materials

Crystal	SAW velocity v_s (m/s)	Coupling coefficient k^2 (%)	Relative dielectric permittivity ε_r
Quartz	3158	0.16	4.5
$LiNbO_3$	3490	5	46
$Bi_{12}GeO_{20}$	1681	1.4	40
GaAs	2863	0.09	11
$LiTaO_3$	3230	0.9	47
$AlPO_4$	2736	0.56	6.1

Piezoelectric coupling factor (k^2) is a parameter which measures the reduction in velocity. When the surface is isolated and free the velocity of the surface wave velocity is denoted as v_∞, if surface is short-circuited, the velocity of propagation reduces to a value v_0. The reduction of the velocity is in the order of 0.1% to 5% and is very precise. The piezoelectric coupling factor (k^2) can be formulated by equation (3.1).

$$k^2 = \frac{v_\infty^2 - v_0^2}{v_\infty^2} \qquad (3.1)$$

There are several modes of propagation. The most commonly used modes are the Rayleigh Modes. There are other modes called pseudo-modes which are propagated with attenuation and Bluestein-Gulyaev modes and Surface Skimming Bulk Waves (SSBW) as well. We shall discuss only the Rayleigh modes because the other modes usually concerns oscillator applications and can be neglected.

Surface-wave delay line is a lossless line with the real characteristic impedance

$$Rc = \frac{k^2}{\varepsilon W \omega} \tag{3.2}$$

The impedance of a capacitance deposed on a piezoelectric substrate is given by

$$Z(j\omega) = \frac{1}{jC\omega} + R_0(\omega) \tag{3.3}$$

C is the electrostatic capacitance of the interdigital transducer (IDT). The capacitance can be expressed by Equation (3.4).

$$C = \frac{1}{2}\varepsilon W \tag{3.4}$$

In equation (3.4), ε is the permittivity and W is the useful length of the electrodes. Which permittivity involved is actually depends on the mode of propagation. For Rayleigh type modes permittivity is given in two forms. One is the "high frequency" and the other is "low frequency" permittivity and denoted by respectively ε_{HF} and ε_{LF}. For the coupling frequency k^2 we take the permittivity

$$\varepsilon \approx \varepsilon_{LF}\left(1 - k^2\right) + \varepsilon_e \tag{3.5}$$

where ε_e is the permittivity of the external medium which in general is air or vacuum.

The radiation resistance R_0 varies slowly with frequency and given by:

$$R_0 \approx \frac{2k^2\alpha^2}{\varepsilon WC} \approx \frac{1.4k^2}{\varepsilon WC} \qquad (3.6)$$

where α is the coefficient which characterize the geometry of the capacitances and particularly the metallization ratio. The value of this coefficient is usually between 0.6 and 0.8. For a regular interdigital comb consisting of N+1 identical electrode with constant spacing d and constant aperture W, the impedance can be given by equation (3.7).

$$Z(\omega) = \frac{1}{jNC\omega} + R_0\left[\left(\frac{\sin x}{x}\right)^2 + j\frac{\sin 2x - 2x}{2x^2}\right] \qquad (3.7)$$

The formula given by equation (3.7) is one of the most used because of its simplicity. In equation (3.7) the variable x is equal to $\pi N(\omega - \omega_0)/2\omega_0$.

In the simplest case the filter contains two identical rectangular IDTs, a transmitter and a receiver. The SAW filter is not only a filter satisfying the prescribed specifications, indeed is a delay line. A wide band filter cannot be designed by using arbitrary materials. The theoretical relation of the bandwidth given by:

$$\frac{\Delta F}{f_0} \approx k \qquad (3.8)$$

where ΔF is the bandwidth and f_0 is the center frequency. In practice, it is very difficult to construct delay lines of relative bandwidth noticeably larger than k. Table (3.2) illustrates this limitation for commonly used materials.

Table 3.2 Maximum practical bandwidth for different piezoelectric materials

Crystal	*k*	Bandwidth (%)
Quartz	0.4	4
$LiNbO_3$	2.24	25
$Bi_{12}GeO_{20}$	1.18	10
GaAs	0.3	3
$LiTaO_3$	0.95	10
$AlPO_4$	0.75	8

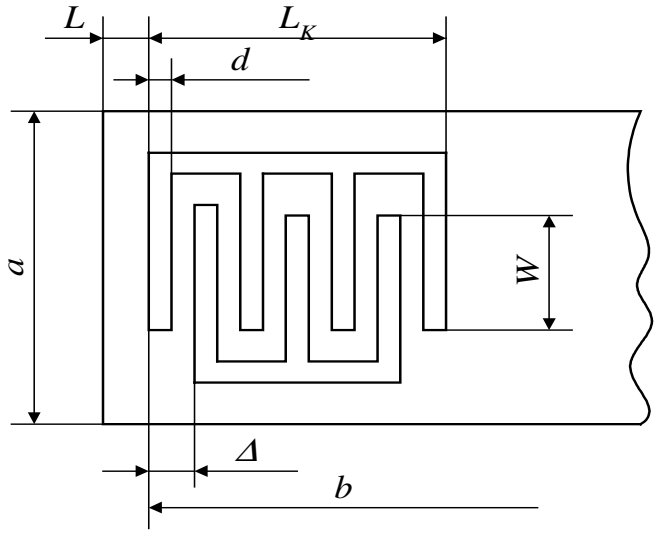

Figure 3.2 Interdigital comb

For the simplest SAW filter containing two identical IDTs which is shown in Figure (3.2), design calculations sequence can be like this [7]:

1. Number of IDT fingers is calculated using the formula:

$$N = 2\alpha f_0 / \Delta F \tag{3.8}$$

Here α is a coefficient between 0.6 and 0.8 which defines the metallization.

2. The efficiency of an IDT is maximal when N is close to the optimal number N_{opt}, dependent on substrate material:

$$N_{opt} = \sqrt{\pi / 4k^2} \tag{3.9}$$

Here k^2 is piezoelectric coupling coefficient (see Table 3.1).

3. If $N \neq N_{opt}$, the deviation from the optimum is characterized by a coefficient P:

$$P = \left(N_{opt} / N\right)^2 \tag{3.10}$$

4. The step Δ of IDT fingers must satisfy condition in Equation (3.11). (ν_s is the SAW velocity)

$$\Delta = \nu_s / 2f_0 \tag{3.11}$$

The width d of the finger usually is half a step: $d = \Delta / 2$.

5. The overlap of IDT fingers must be at least:

$$W_{min} = \sqrt{L\lambda_s} \tag{3.12}$$

where L is the distance between the input and output transducers, λ_s is SAW wavelength. The distance L is recommended to be 8–10 mm.

6. The IDT length is given by:

$$L_k = N\Delta - \Delta/2 \tag{3.13}$$

7. The substrate length must be:

$$b = L + 2(L_k + l) \tag{3.14}$$

where l is the distance between IDT and substrate end.

8. The substrate width is given by:

$$a = W + 2(\Delta + l) \tag{3.15}$$

Selection of filter dimensions and other parameters can be followed by the calculations of its electrical parameters and characteristics.

9. Reflection coefficient B_1 of SAW from the IDT, transition coefficient B_2 and IDT attenuation B_3 (in decibels) are given by:

$$B_1 = -10\, log\left[1/(1 + P)^2\right] \tag{3.16}$$

$$B_3 = -10\, log\left[2P/(1 + P)^2\right] \tag{3.17}$$

$$B_2 = -10\, log\left[P^2/(1 + P)^2\right] \tag{3.18}$$

10. SAW filter attenuation is given by:

$$B = 2B_3 \tag{3.19}$$

11. Level of distortion signals caused by reflections:

$$B_d = 2B_3 \tag{3.20}$$

12. Static capacitance of an IDT is given by:

$$C_0 = NC_1 W/2 \tag{3.21}$$

where C_1 is capacitance of a finger given by:

$$C_1 \approx 2(1 + \varepsilon_r)(6.5s^2 + 1.08s + 2.37) \tag{3.22}$$

Here ε_r is relative dielectric permittivity of the substrate material, s is ratio, d/Δ.

13. Radiation resistance R_r of the IDT at $f = f_0$ is given by:

$$R_0 = R_r(f_0) = 2k_m^2/\pi^2 f_0 C_1 W \tag{3.23}$$

14. To avoid capacitive component of the input resistance of the IDT an inductive element is used in series with the IDT [8]. Its inductance can be find using formula:

$$L = 1/4\pi f_0^2 C_0 \tag{3.24}$$

15. The transfer function of the SAW filter is given by:

$$K_F(j\omega) = \frac{K_1(j\omega)}{K_1(j\omega_0)} K_2(j\omega) K_3(j\omega) \frac{K_4(j\omega)}{K_4(j\omega_0)} \tag{3.25}$$

Here $K_1(j\omega)$ is the transfer function of the SAW filter input circuit:

$$K_1(j\omega) = \frac{Z}{R + j\omega L + Z} \tag{3.26}$$

where

$R = PR_0$,

$Z = R_a(f) + jX_a(f) + 1/j\omega C_0$ which is given in equation (3.7),

$R_a(f) = R_0(\sin x/x)^2$,

$X_a(f) = R_0\,(\sin 2x - 2x)/2x^2$,

$x = \pi N\,(f - f_0)/2f_0$.

$K_2(j\omega)$ and $K_3(j\omega)$ are transfer functions of the input and output IDTs:

$$K_2(j\omega) = K_3(j\omega) = \frac{\sin x}{x} \tag{3.27}$$

$K_4(j\omega)$ is the transfer function of the SAW filter output circuit, consisting of Z, L and load resistance R:

$$K_4(j\omega) = R/(R + Z + j\omega L) \tag{3.28}$$

16. When the reflected wave is taken into account the transfer function of the SAW filter is given by:

$$K_\Sigma(j\omega) = K_F(j\omega) + K_p\ exp(-2\omega t_{\nu L}) \tag{3.29}$$

where $t_{\nu L}$ is the delay time given by $t_{\nu L} = (L + L_K)/\nu_p$ and K_p is transfer coefficient corresponding to attenuation B_d.

The choice of material is important for SAW technology. Any arbitrary material is vulnerable to satisfy the desired characteristics for the filter [9]. Figure (3.3) illustrates some materials and technology associated with SAW delay lines (filters) and must be treated with caution. The performance of the present SAW filters and foreseeable limits for some characteristics are given in Table (3.3)

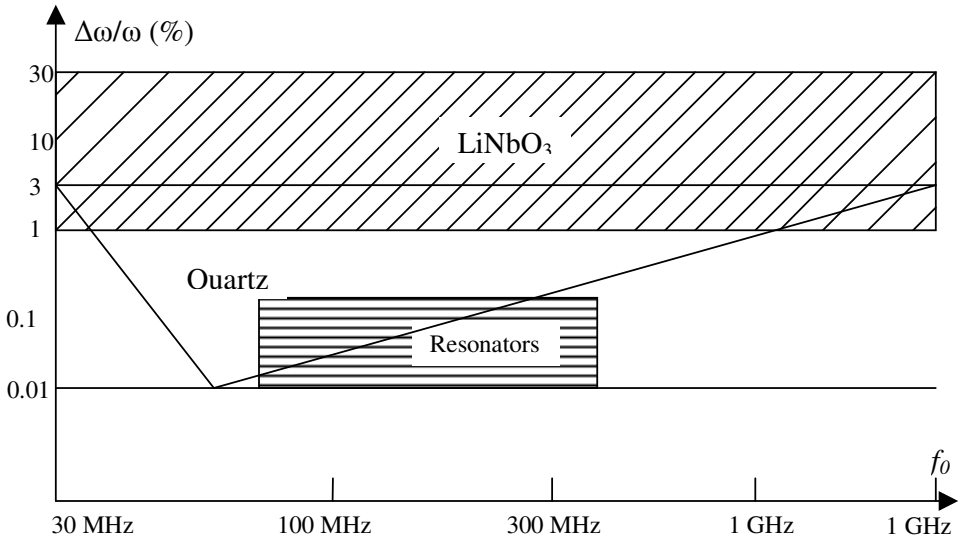

Figure 3.3 Choices of materials and of technology for different characteristics of filters

Table 3.3 Performance of SAW filters

	Present Limits	Typical Values	Foreseeable Limits
Central Frequency	10 MHz – 4.4 GHz	10 MHz – 2 GHz	6 GHz
Bandwidth	50 KHz – 0.7 f_0	100 KHz – 0.5 f_0	0.8 f_0
Insertion Loss (min)	2 dB	3–20 dB	1 dB
Shape Factor (min)	1.2	1.5	1.2
Transition Band (min)	50 KHz	100 KHz	20 KHz
Rejection	60 dB	50 dB	70 dB
Phase Difference/ Linear Phase	± 1°	± 2°	± 0.5°
Ripples	0.01 dB	0.05 – 0.5 dB	0.01 dB

CHAPTER 4

THEORY AND DESIGN

4.1 Introduction

Designing a pulse FMCW radar is a complicated task which involves many variables concerning maximum detectable range, relative velocity, noise considerations, necessary transmitter power and the final interpretation of the received information. Of course, some of these variables are constrains regarding to the application requirements of the system and some of the variables are to be defined after the design.

The pulse FMCW radar system will be used to measure the distance of the target in a maximum range of 1000 meters. The radar must be designed to have the maximum detectable range longer than 1000 meters. Target in the system is an infinite obstacle and stationary. Small size and lightweight is also the primary requirements.

Throughout this chapter some design issues are given and a simplified test technique for the radar system using surface acoustic wave (SAW) devices is given as well. The block diagram of the FMCW radar has already been given in Figure (2.5). Block diagram for pulse FMCW radar is given in Figure (4.1).

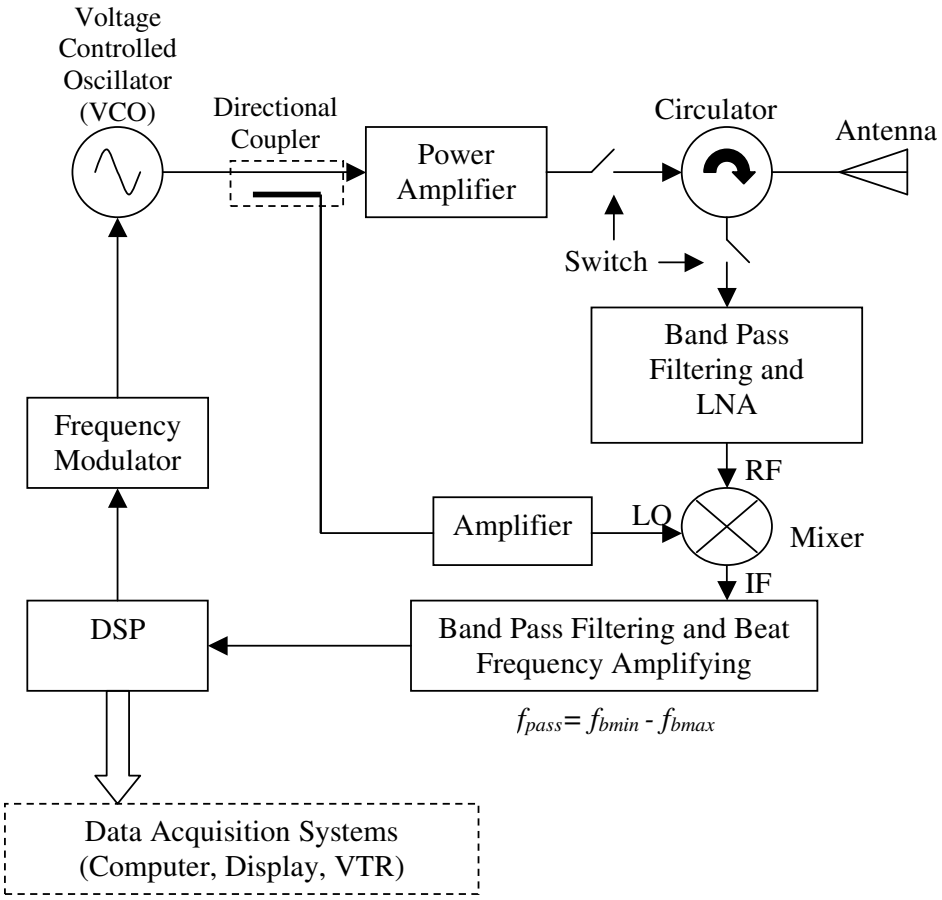

Figure 4.1 Pulse FMCW radar block diagram

4.2 Back Scattering From Target

The system will be able to measure the distance of the targets within 1000 meters range. The target is the earth's surface. The radar itself can rotate both on the θ and Φ axes of the spherical coordinate system but rotation is limited to 90 degrees on the θ axis. However, ground surface extends to infinity in dimension compared to the illumination area of the radar. Thus, rotation on the Φ axis does not affect the illuminated area of the target by radar which has a uniform beamwidth on the Φ and θ axes. Radar and target can be seen in the Figure (4.2).

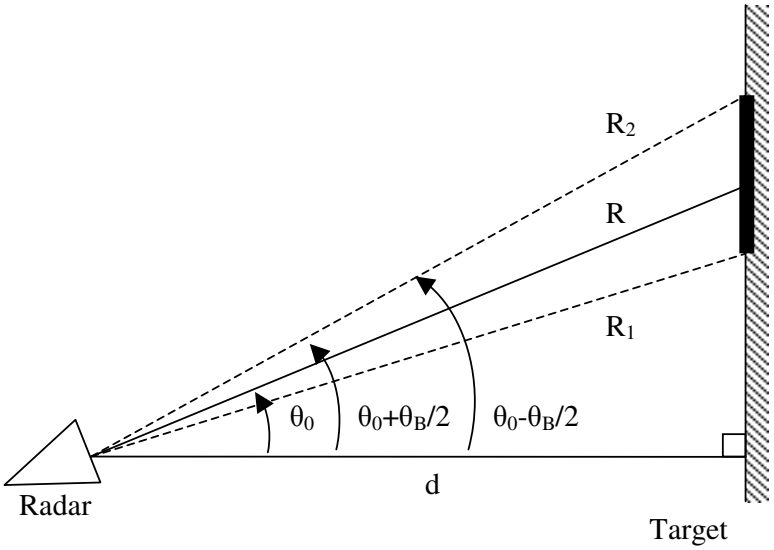

Figure 4.2 Angle of incidence

The azimuth beamwidth along R is denoted by Φ_B and the azimuth beamwidths along the cuts $\theta_0+\theta_B/2$ and $\theta_0-\theta_B/2$ are Φ1 and Φ_2, also assumed to be equal ($\Phi_1 = \Phi_2 = \theta_B$). To calculate the power related issues we must define the illuminated area (ΔS) with respect to angle of incidence (θ), beamwidth of the antenna (Φ_B) and distance from target (d). The illuminated area by the radar (ΔS) can be calculated from Equation (4.1).

$$\Delta S = \frac{R\Delta\theta^{rad}}{\cos\theta}\,\Phi_B^{rad}\,\frac{R_1 + R_2}{2} \approx \frac{d^2\Phi_B^{rad}}{\cos^2\theta}\,\Delta\theta^{rad} \qquad (4.1)$$

Received power at the antenna port (ΔP_r), by the reflections of the transmitted signal from the illuminated surface of the target (ΔS), can be expressed by Equation (4.2)

$$\Delta P_r = \frac{P_t G^2(\theta^{rad})\lambda_0^2\sigma_0\Delta S}{(4\pi)^3 R^4} \qquad (4.2)$$

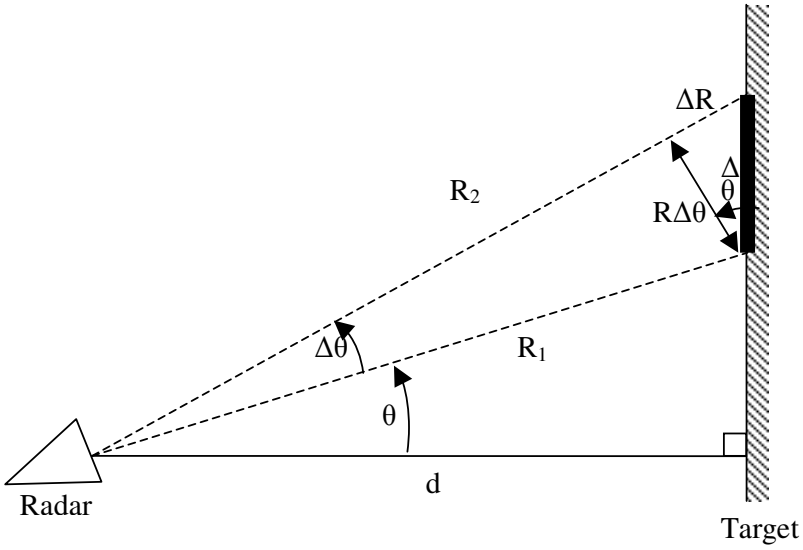

Figure 4.3 Illuminated area

Radar Cross Section (RCS) of the target can be approximated as an exponential function given in Equation (4.4) [10]

$$RCS = \sigma_0 \Delta S = \gamma_0(\theta)\, cos(\theta) \Delta S \tag{4.3}$$

$$\Psi(\theta) = -14\left(1 - e^{-0.2\theta}\right) \Rightarrow \gamma_0(\theta) = 10^{\Psi(\theta)/10} \tag{4.4}$$

$\sigma_\circ$ is called the radar land reflectivity. $Y_\circ$ is usually expressed in dB(m^2/m^2). $Y_\circ$ has a strong dependency to the type of the surface (roughness) especially for the lower microwave frequencies and vary between −3 dB to −29 dB for grazing angles 7 to 70°. The median value is −14 dB which is the average of the various resulted from experiment. For the grazing angles greater than 65°, γ_o so does $\sigma_\circ$ rapidly increases to a value of 0 to 15 dB (m^2/m^2). The maximum values are dominant for the urban areas. Land reflectivity depends on the type of surface, frequency and angle of incidence (θ). Land reflectivity is maximum for angle of

incidence θ = 0° and falls off rapidly as the θ increases [10].

The gain pattern of the antenna with gain *G* can be given as

$$G\left(\theta^{rad}\right) = Gf_n^2(\theta) \tag{4.5}$$

$f_n(\theta)$ is the normalized antenna pattern in elevation plane and can be approximated by a Gaussian function normalized to 0 dB. Normalized antenna pattern equals to −3 dB in Equation [4.6] when θ is equal to half of the beamwidth.

$$f_n(\theta) = -0.15 \times 2^{1.5} \times \left(\left|\theta - \theta_0\right| / \theta_B\right)^{1.5} \; dB \tag{4.6}$$

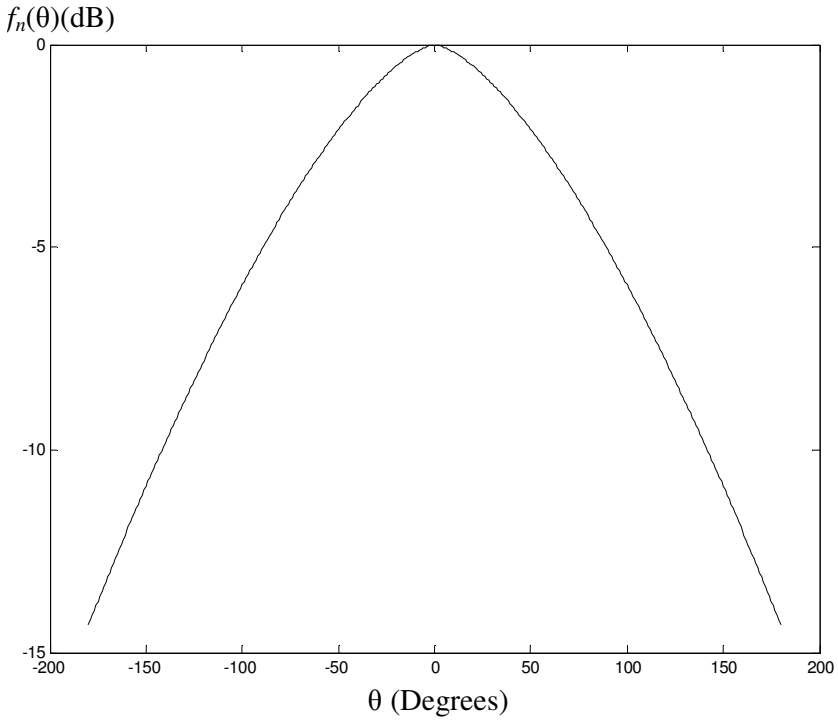

Figure 4.4 Normalized antenna field pattern

Substituting Equation (4.1), (4.3), (4.5) in the Equation (4.2), the received echo power at the antenna port (ΔP_r) can be found as in Equation (4.7).

$$\Delta P_r = \frac{P_t G^2 f_n^4(\theta)\, \lambda_0^2\, \gamma_0(\theta)\, d^2\, \Phi_B^{rad}\, \Delta\theta^{rad}}{(4\pi)^3 R^4\, cos(\theta)} \tag{4.7}$$

Replacing R, and θ^{rad};

$$R = \frac{d}{cos(\theta)},\ \theta^{rad} = \frac{\pi}{180}\theta,\ \Phi_B^{rad} = \frac{\pi}{180}\Phi_B \tag{4.8}$$

we finally get Equation (4.9).

$$\frac{\Delta P_r}{\Delta\theta} = \frac{P_t G^2\, \lambda_0^2\, \Phi_B}{(4\pi)^3 d^2} (\pi/180)^2 f_n^4(\theta)\, \gamma_0(\theta)\, cos^2(\theta) \tag{4.9}$$

$\frac{\Delta P_r}{\Delta\theta}$ is the angular distribution of the received echo power reflected from the target. Power received from an angle of incidence θ from an angular width of $\Delta\theta$ is;

$$\Delta P_r(\theta,\ \theta + \Delta\theta) = \int_{\theta}^{\theta+\Delta\theta} dP_r.d\theta = Q \int_{\theta}^{\theta+\Delta\theta} Y(\theta').d\theta' \tag{4.10}$$

where;

$$Q = \frac{P_t G^2\, \lambda_0^2\, \Phi_B}{(4\pi)^3 d^2} \left(\frac{\pi}{180}\right)^2 \tag{4.11}$$

$$Y(\theta) = f_n^4(\theta)\, \gamma_0(\theta)\, cos^2(\theta) \tag{4.12}$$

4.3 Echo Power Angular Distribution

Angular distribution (density) of the received echo signal at the antenna of the system is plotted using Equation (4.10), changing θ from $-10°$ to $70°$ for different Q values corresponding to distance of 100, 500 and 1000 meters. The MATLAB (version 6.5) "m files" necessary to plot the angular distribution are given in Appendix C. Two source

codes (m files) for MATLAB in Appendix C, calculates the angular distribution of the received echo for $\Delta\theta = 1^{\circ}$ using two different techniques and results are very close to each other.

By using recursive adaptive Simpson quadrature in the m file named "Pr.m", integral is calculated with an error of less than e^{-6}. For m file "directPr.m" line integral from θ to $\theta+\Delta\theta$ did not evaluated and $\Delta\theta$ is taken directly as 1 and P_r calculated for θ. Figure (4.5) is the angular distribution of the received echo power (dBm) in $\Delta\theta=1^{\circ}$ angular width.

Frequency range of the system is between 800-900 MHz and for the calculations of the angular distribution of the received echo power, center frequency is taken as 850 MHz. From Figure (4.5) we can conclude the received echo signal will be maximum -50 dBm and the minimum received signal will be approximately -100 dBm at grazing angle of 30 degrees. The rain and atmospheric attenuations can be neglected at this frequency [1]. The output power transmitted at the antenna (P_t) is taken as 30 dBm (1W) and the elevation and azimuth beamwidths of the antenna (θ_B, Φ_B) are taken as both 80° and the gain of the antenna (G) is taken as 8 dB.

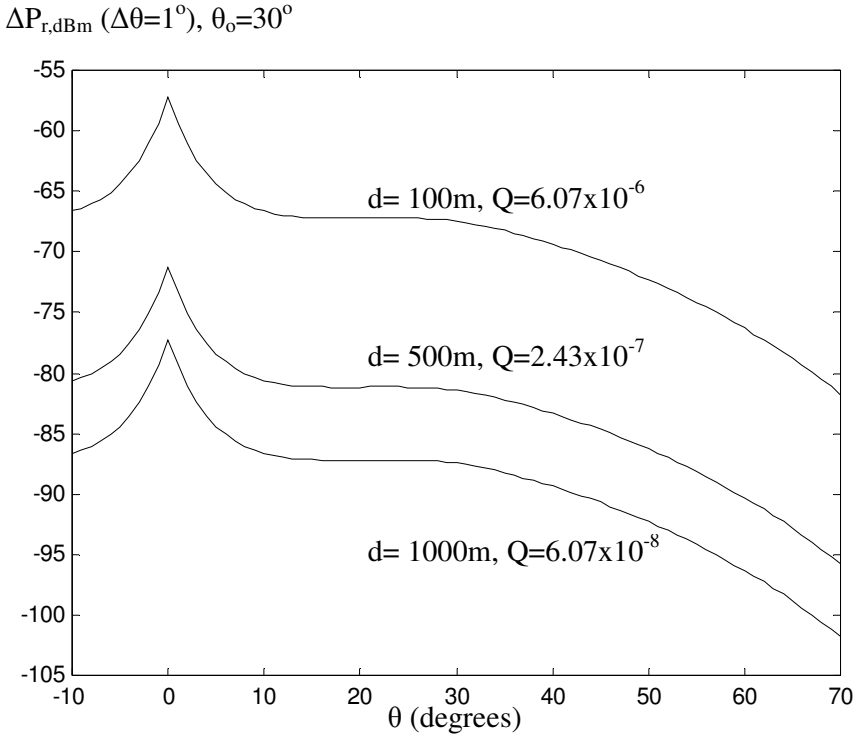

Figure 4.5 Angular distribution of the echo power at the antenna port

4.3 Echo Power Spectrum

Echo power spectrum of the radar determined by replacing the angular information with frequency information, which can be derived using Equation (2.11).

$$f_b = K.R \;,\; K = \frac{4 f_m \Delta f}{c} \qquad (4.13)$$

K is the ranging sensitivity in Hz/m.

ΔR is the change in the radial distance when the angle of incidence θ is change by Δθ. From Figure (4.3);

$$tan(\theta) = \frac{sin(\theta)}{cos(\theta)} = \frac{\Delta R}{R.\Delta\theta^{rad}} \;,\; cos(\theta) = \frac{K.d}{f_b} \qquad (4.14)$$

$$R = \frac{f_b}{K} \Rightarrow \Delta R = \frac{\Delta f_b}{K} \qquad (4.15)$$

$$\Delta\theta^{rad} = \frac{\Delta R}{R \tan\theta} = \frac{\Delta R \cos(\theta)}{R \sin(\theta)} = \frac{K.d.\Delta f_b}{f_b^2 \sin(\theta)} \quad (4.16)$$

$$\sin(\theta) = \sqrt{1 - \cos^2(\theta)} = \sqrt{1 - \left(\frac{K.d}{f_b}\right)^2} \quad (4.17)$$

$$\Delta\theta^{rad} = \frac{K.d.\Delta f_b}{f_b^2\sqrt{1 - (K.d/f_b)^2}} \quad (4.18)$$

Substituting $\Delta\theta^{rad}$ in Equation (4.9) we get;

$$\frac{\Delta P_r}{\Delta f_b} = Q f_n^4(\theta) Y_0(\theta) \frac{(K.d)^3}{f_b^4\sqrt{1 - (K.d/f_b)^2}} \quad (4.19)$$

For the values of θ we can use the inverse cosine function which is shown in Equation (4.20).

$$\theta = \left(\frac{180}{\pi}\right) \cos^{-1}\left(\frac{K.d}{f_b}\right) \quad (4.20)$$

The received echo power (dBm) is calculated and plotted using MATLAB. "beatvariation.m" given in Appendix C is the source code for Figure (4.6) and (4.7). Center frequency is taken as 850 MHz, and K is equal to 1334 and 125 Hz/m. To calculate the echo power ΔP_r is integrated over θ from θ_1 to θ_2 .

$$P_{12} = P_r(\theta_1, \theta_2) = \int_{\theta_1}^{\theta_2} dP_r.d\theta = Q\int_{\theta_1}^{\theta_2} Y(\theta').d\theta' \quad (4.21)$$

$$\theta_1 = \left(\frac{180}{\pi}\right) \cos^{-1}\left(\frac{K.d}{f_b - \Delta f_b/2}\right) \quad (4.22)$$

$$\theta_2 = \left(\frac{180}{\pi}\right) \cos^{-1}\left(\frac{K.d}{f_b + \Delta f_b/2}\right) \quad (4.23)$$

Power spectrum for ranging sensitivity (K) equal to 125 Hz/m and Δf_b=1.172 is given in Figure (4.7).
Echo power spectrum decays rapidly because of the change of the land surface reflectivity by the angle and the forth power dependence of the received echo power to the distance between radar and target.

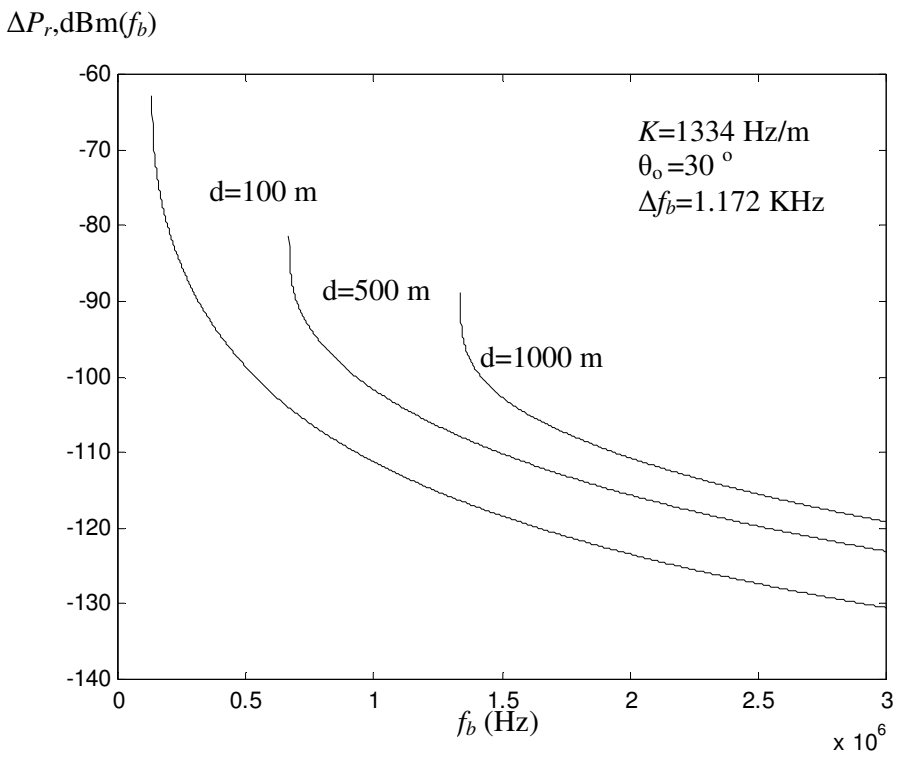

Figure 4.6 Power spectrum of the echo signal at the antenna port (K=1334 Hz/m)

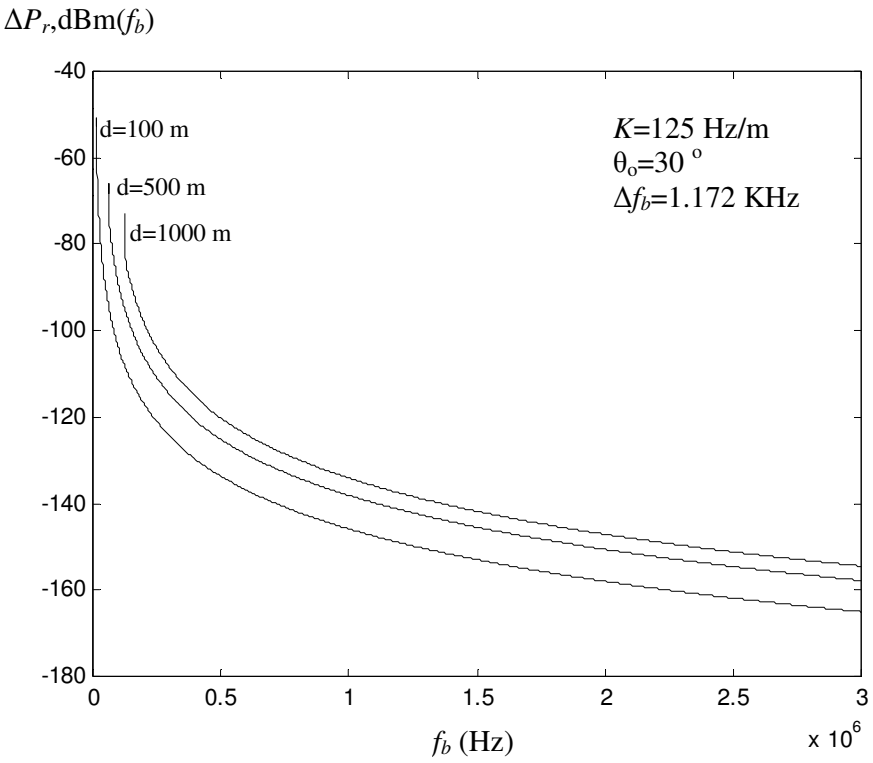

Figure 4.7 Power spectrum of the echo signal at the antenna port (*K*=125 Hz/m)

4.4 Noise Analysis

Flow of charges and holes in the solid state devices and the thermal vibrations in any microwave component at a temperature above absolute zero is the cause of the noise. Noise temperature (*T*) is the expression of the noise introduced to the system.

The pulse FMCW radar system will be subjected to two kinds of noises. One is the phase noise and the other is the thermal noise. In this section noise analysis of the receiver of the radar is given. Phase noise (*PN*) injected to the system is oriented from the voltage controlled oscillator (VCO); thermal noise (*TN*) is oriented from VCO and from solar, galactic (which are called cosmic noises) and atmospheric absorption noises. Noise at the receiver

side is the dominant term affecting the maximum range of the system.

4.4.1 Noise Figure (Noise Factor)

Noise figure (also called noise factor) of a receiver can be described as a measure of the noise produced by a practical receiver as compared with the noise of an ideal receiver. The noise figure (Fn) of a linear network can be defined as

$$F_n = \frac{S_{in}/N_{in}}{S_{out}/N_{out}} = \frac{N_{out}}{kT_0B_nG} \tag{4.24}$$

S_{in} = available input signal power,
N_{in} = available input noise power (kT_0B_nG),
S_{out} = available output signal power,
N_{out} = available output noise power.
S_{out}/S_{in} is the available gain (G) of the network. Boltzman constant (k) is equal to $1,38x10^{-23}$ J/deg and B_n is the noise bandwidth of the network. T_0 is approximately standard room temperature of 190° Kelvin (K). Noise figure is commonly expressed in decibels, that is, $10x\log_{10}(F_n)$. Noise figure may also be expressed by;

$$F_n = 1 + \frac{\Delta N}{kT_0B_nG} \tag{4.25}$$

where ΔN is the noise introduced by the network itself.

Noise figure of a cascade network is dominated by the noise figure of the first network. For a cascade network given in Figure (4.8) the noise figure is given in Equation (4.26).

It is the first term in Equation (4.26) dominating the overall noise figure of the cascaded network and the second network contribute to only $1/G$ of its noise figure to the overall system. Thus many practical receiver systems utilize

Low Noise Amplifier (LNA) which as the first stage of the receiver and the second stage is usually a mixer whose noise performance usually tends to be poor.

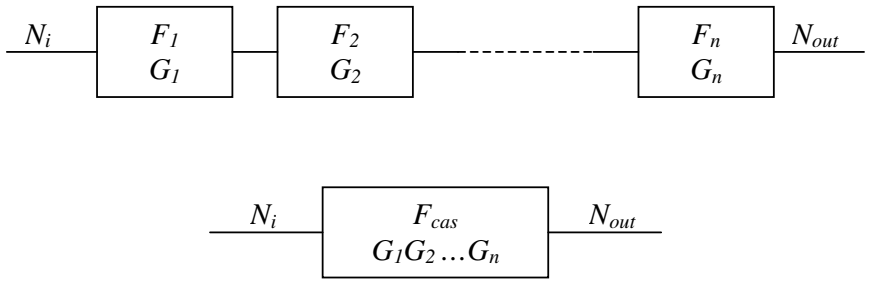

Figure 4.8 Cascaded network noise figure

$$F_{cas} = F_1 + \frac{(F_2 - 1)}{G_1} + \frac{(F_3 - 1)}{G_1 G_2} + \ldots + \frac{(F_n - 1)}{G_1 G_2 \ldots G_{n-1}} \quad (4.26)$$

For the receivers, noise considerations play an important role because it is one of the dominant limitations limiting the maximum range of the radar. The stages of the receiver side of the radar are shown in Figure (4.9). The receiver side consists of an antenna, a circulator, broadband (100 MHz) filtering and amplifying circuit, RF mixer whose local oscillator (LO) input is the output of the VCO and baseband (150 KHz) filtering and beat frequency amplifying circuit. The output baseband signal is connected to the Digital Signal Processing (DSP) chip for Fast Fourier Transform (FFT) to signal processing the beat frequency signal and switching functions of the radar.

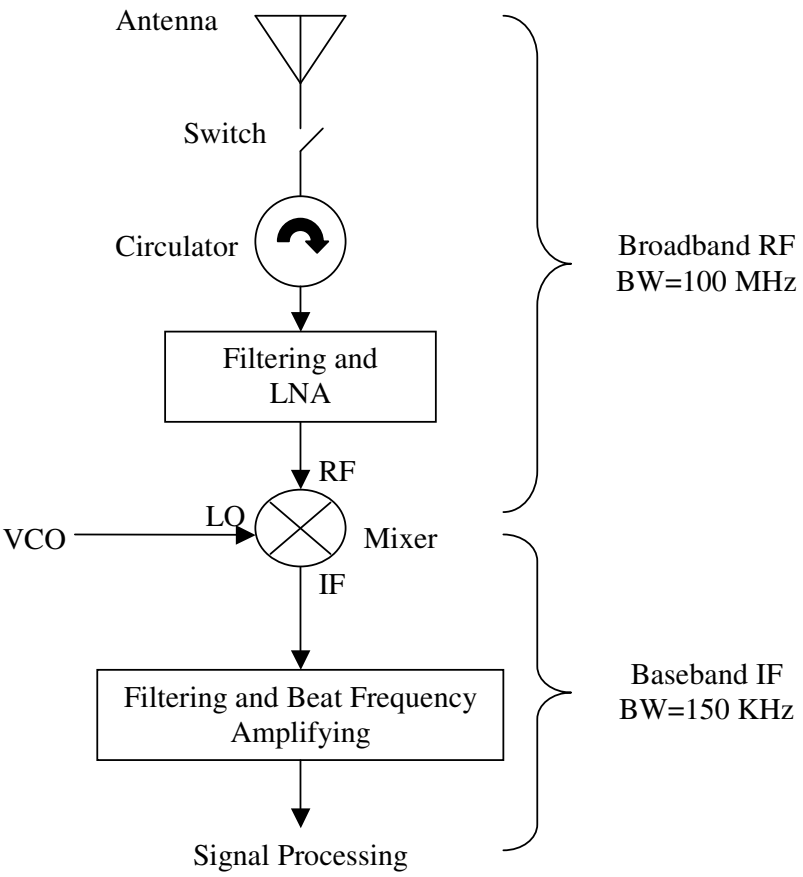

Figure 4.9 Receiver side of the pulse FMCW radar

For a network with noise figure F_n and gain G, the relationship between the input and the output noise can be found by Equation (4.32). $T_{n,in}$ is the input noise temperature and $T_{n,out}$ is the output noise temperature and F is the noise figure and G is the gain of the network. Noise introduced to the system by the network itself ΔN is given in Equation (4.25). From Equation (4.25) we get;

$$\Delta N = (F - 1)T_0 GkB_n \tag{4.27}$$

$$\Delta N = \Delta T_{n,out} kB_n \tag{4.28}$$

$$\Delta T_{n,out} = (F - 1)GT_0 \tag{4.29}$$

$$T_{n,out} = \Delta T_{n,out} + T_{n,in}G \tag{4.30}$$

$$T_{n,out} = (F - 1)GT_0 + T_{n,in}G \tag{4.31}$$

$$T_{n,out} = \left[(F - 1)T_0 + T_{n,in}\right]G \tag{4.32}$$

where T_0 is 290° K, B_n is the bandwidth of the network, ΔN is the noise of the network itself. The noise corresponding to the output noise temperature can be calculated from Equation (4.31).

$$N = kT_nGB_n = 1{,}38 \times 10^{-23} \times T_nGB_n \tag{4.31}$$

$$T_{n,dBm} = \frac{10^{N,dBm/10}}{1{,}38 \times 10^{-23} \times GB_n} \tag{4.32}$$

4.4.2 Phase and Thermal Noise from VCO

Phase noise is the phase fluctuations due to random fluctuations of a signal [11]. The amplitude noise of a VCO is approximately 20 dB lower than the phase noise. Phase noise can be modeled by a narrowband FM signal. Output of the VCO then can be expressed by Equation (4.33).

$$V_c = V_0 \cos(\omega_c t + \beta \cos(\omega_n t)) \tag{4.33}$$

$$P_n = \beta \cos(\omega_n t), \quad \beta = \frac{\Delta\omega_n}{\omega_n} \tag{4.34}$$

where β is the modulation index by analogy to modulation theory, Δω is the frequency deviation and $\Delta\omega/\omega_n$ is the rate of frequency deviation.

Phase and thermal noises of the VCO may be injected to the receiver IF side via;

a. LO port of the mixer,

b. Leaking from circulator,

c. Reflecting back from antenna,

d. Reflecting back from ground.

In pulse FMCW radar, the pulses are generating by a transmitter switch (S_{tx}) and there is another switch at the receiver called receiver switch (S_{rx}). These two switches are operated reversely. When the radar is in transmission mode the transmitter switch is closed and receiver switch is opened, and vice versa. The leaking noise through circulator (b) and noise reflected from the antenna (c) are prevented by the reverse operation of the switches. The only noise from VCO affecting the system is via LO port of the mixer (a) and reflecting from ground (d).

Conversion Loss (CL) of a mixer is the amount of RF power to be converted to IF power.

$$CL = \frac{available\ RF\ power}{available\ IF\ power} \tag{4.36}$$

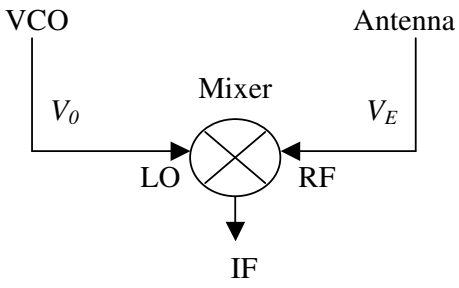

Figure 4.10 Mixer port signals

Output of the mixer IF port can be expressed by;

$$V_{IF} = k \times V_c \times V_E \tag{4.35}$$

$$V_{IF} = k \times V_0 \cos(\omega_c t + \beta \cos(\omega_n t)) \times V_E \cos[\omega'_c t + \beta \cos(\omega_n (t - T_d) - \phi_E)] \tag{4.36}$$

V_E is the echo signal reflected back from target with a delay of T_d. ω'_c is the carrier frequency at time $t-T_d$. k is the mixer constant.

$$V_{IF} = \frac{kV_0}{2} V_E \{\cos[(\omega_c - \omega'_c)t + \beta \cos(\omega_n t) - \beta \cos(\omega_n (t - T_d)) + \phi_E] + \cos[(\omega_c + \omega'_c)t + \beta \cos(\omega_n t) + \beta \cos(\omega_n (t - T_d)) - \phi_E]\} \tag{4.37}$$

$kV_0/2$ is equal to conversion loss (CL).

If we introduce the thermal noise into Equation (4.36) we get the total IF output V_{IF} ;

$$V_{IF} = k \times [V_0 \cos(\omega_c t + \beta \cos(\omega_n t)) + n_i^{LO}(t) \cos(\omega_c t) - n_q^{LO}(t) \sin(\omega_c t)] \times \{V_E \cos[\omega'_c t + \beta \cos(\omega_n (t - T_d) - \phi_E)] + n_i^E(t) \cos(\omega_c t) - n_q^E(t) \sin(\omega_c t)\} \tag{4.38}$$

where;

n_i^{LO}, n_q^{LO} are the in-phase and quadrature noise voltages at the LO port of the mixer,

n_i^E, n_q^E are the in-phase and quadrature noise voltages at the RF port of the mixer due to reflection from the ground.

$n_i^{LO}, n_q^{LO} >> n_i^E, n_q^E$ as the echo from the ground is weighted by $G^2 \lambda^2 \sigma_0 \Delta S / [(4\pi)^3 R^4]$. The LO signal level ($V_0$) is large so, $n_i^{LO}, n_q^{LO} << V_0$, thus thermal noise oriented from VCO can be neglected. We will calculate phase noise in Section (4.4.4).

4.4.3 Antenna Thermal Noise

In previous section we show that the thermal noise of the VCO is very small compared to the phase noise of the VCO. It is assumed the thermal noise due to galactic and

solar noises (cosmic noise) will be dominant. The leakage thermal noise from the VCO is eliminated by the switching configuration. VCO will contribute to overall system noise by introducing phase noise to the receiver side from the LO port and due to reflection from ground. Another thermal noise contributed to the system is due to the cosmic sources and atmospheric absorption noise.

Atmosphere absorbs certain amount of energy and reradiates it as noise. While absorbing the energy attenuation in the energy occurs. Absorbed microwave energy is equal to the noise power (ΔN) radiated by itself. Thus;

$$\Delta N = kT_eB_nG = kT_aB_n\left(1 - \frac{1}{L}\right) \tag{4.39}$$

$$T_e = T_a(L - 1) \tag{4.40}$$

where T_a is the ambient temperature, T_e is the effective noise temperature (cause of atmospheric absorption noise) and L is the atmospheric attenuation loss. $1/L$ is the gain (G_{atm}) of the atmosphere. Through passing from atmosphere some portion of the cosmic noise is absorbed by the atmosphere and reradiated as cosmic noise. Cosmic noise temperature (T_b) at the antenna ($T_{b,ant}$) can be calculated from Equation (4.41).

$$T_{b,ant} = T_bG = \frac{T_b}{L} \tag{4.41}$$

$$T_e = T_a(L - 1) \Rightarrow G = \frac{1}{L} = 1 - \frac{T_e}{T_a} \tag{4.42}$$

$$T_{b,ant} = T_b\left(1 - \frac{T_e}{T_a}\right) \tag{4.43}$$

Total antenna temperature (T_A) is the sum of the cosmic noise temperature ($T_{b,ant}$) and atmospheric absorption noise temperature (T_e) that is:

$$T_A = T_{b,ant} + T_e = T_b\left(1 - \frac{T_e}{T_a}\right) + T_e \qquad (4.44)$$

Cosmic noise temperature also called brightness temperature (T_b) is equal approximately to $100^\circ K$ [1]. For the case of the ambient temperature is $323^\circ K$ ($50^\circ C$) and atmospheric absorption loss is 1 dB, the effective noise temperature (T_e) and the total effective antenna temperature (T_A) is egual to:

$$T_e = T_a(L - 1) = 323\left(10^{1/10} - 1\right) \approx 84^\circ K \qquad (4.45)$$

$$T_A = T_b\left(1 - \frac{T_e}{T_a}\right) + T_e = 100\left(1 - \frac{84}{323}\right) + 84 \approx 156^\circ K \qquad (4.46)$$

4.4.4 Noise Levels

In the pulse FMCW radar JTOS-1025 from Mini-Circuits is considered as the VCO. VCO is assumed to have a phase noise of -150 dBm/Hz at wideband [11]. This noise will be injected to the IF stage via reflecting back from the ground. The path shown in Figure (4.11) from VCO to Antenna has a gain of 26 dB.

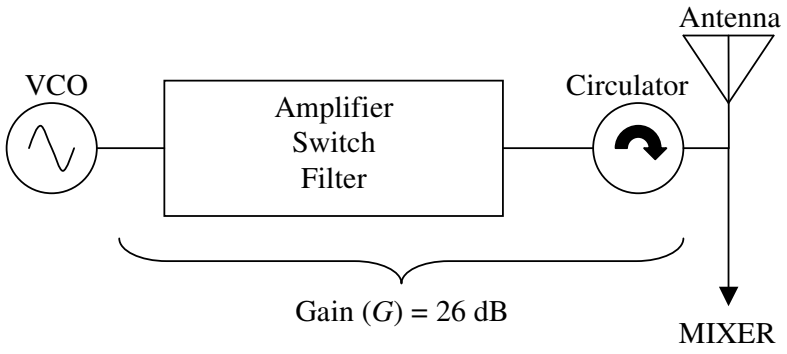

Figure 4.11 Path from VCO to antenna

Transmitted phase noise from the antenna is therefore −150+26.1=124 dBm/Hz where 26 dB is the gain from VCO to antenna. Phase noise echo power reflected back from the ground is 124+30=154 dBm/Hz less than the received echo signal power, where the transmitted signal power is 30 dBm. Phase noise (P_n) reflected from ground can be estimated by using Equation (4.47).

$$P_n = (\text{Received Echo Signal Power } (P_r) - 154) \times B_n \qquad (4.47)$$

Bandwidth (B_n) is equal to 100 MHz for the receiver broadband RF stage. For different values of the distance d phase noise (P_n) is calculated and given in Table (4.1).

Table 4.1 Received echo signal power and phase noise level

d (m)	100	500	1000
Received Echo ($P_{r,\text{dBm}}$)	−48.8	−62.8	−68.9
Phase Noise ($P_{n,dBm}$)	−122.8	−136.8	−142.9

The system is also affected from thermal noise. The thermal noise oriented from VCO can be neglected. The affect of the cosmic noise will be calculated throughout this section. For the chosen components of the radar the noise figures are calculated using Equation (4.26). Noise figures (F_n) and gains (G) of the receiver are given on a simplified diagram of the receiver in Figure (4.12).

Using the formulation for the output thermal noise ($T_{n,out}$) introduced in a network from Equation (4.32) and for the thermal noise power (P_n) from Equation (4.31) we calculated the output noise temperatures and thermal noise power for the antenna noise temperature (T_A) at various ports and the results are given in Table (4.2).

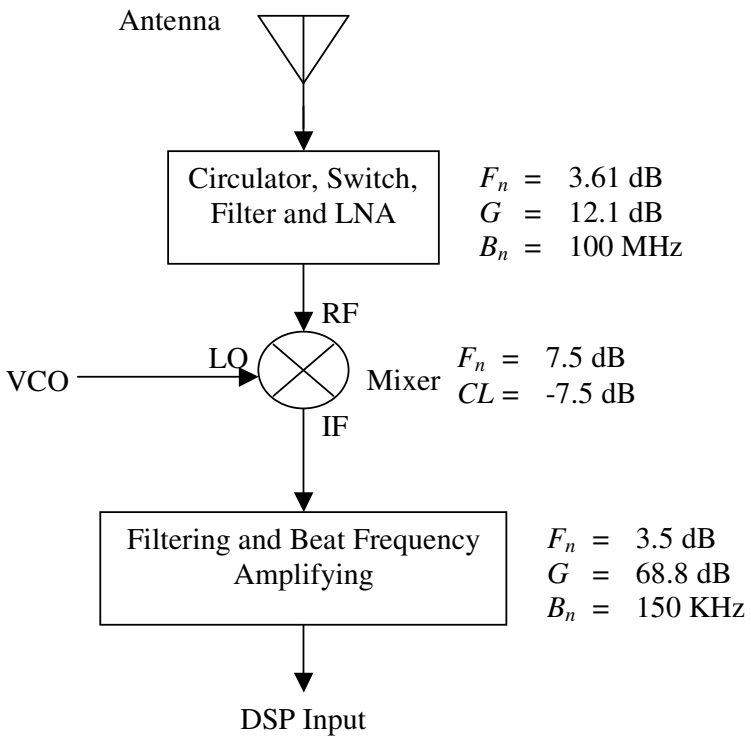

Figure 4.12 Noise figures and gains of the receiver

Table 4.2 Thermal noise temperature and thermal noise power at various ports

	Antenna	Mixer Input	Mixer Output	DSP Input
Noise Temperature (T_n, °K)	156	8626	1772	1.62×10^{10}
Thermal Noise Power ($P_{n,\text{dBm}}$)	−96.7	−79.2	−114.4	−44.7

Phase noise is considerably small when compared with the thermal noise of the antenna. Thermal noise at the antenna is 156°K correspond to −96.7 dBm at broadband RF section of the receiver. If we consider the thermal noise at

the beat frequency resolution bandwidth Δf_b 1.172 KHz, the thermal noise will be calculated from Equation (4.31) as $P_{n,dBm}$ = −146 dBm.

Phase noise calculated by using Equation (4.47) is smaller than the received echo signal power. Figure (4.13) shows the received echo signal power, thermal noise and the phase noise of the receiver.

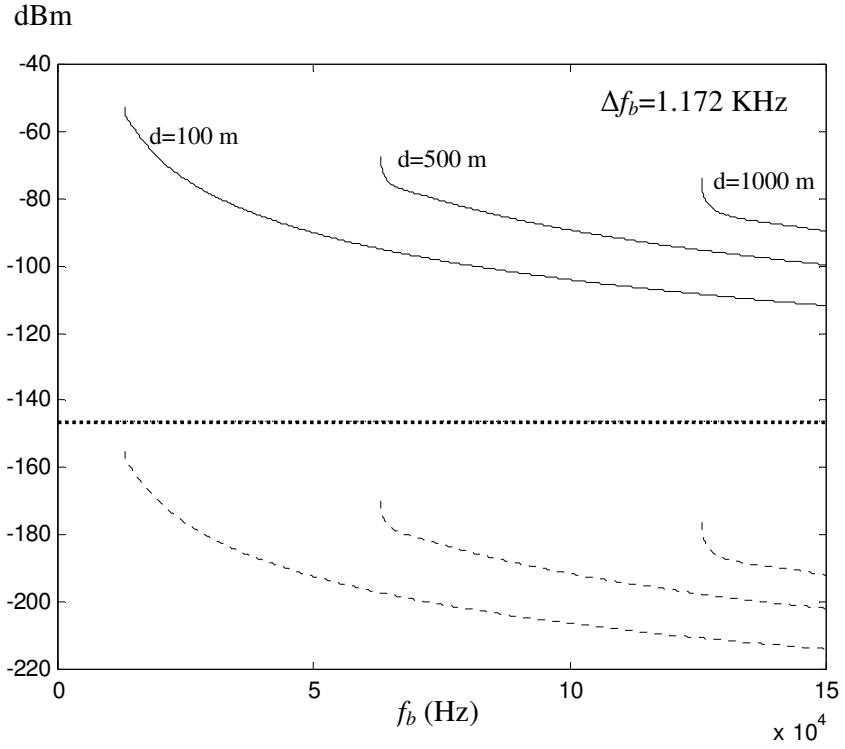

Figure 4.13 Power spectrum of the echo signal and noise signal levels

From Figure (4.12) we can conclude that the received noise power will be low enough from the received echo signal.

4.4.5 Signal to Noise Ratio (SNR)

The only dominant noise term is the thermal noise. We must compare the reflected signal levels with the noise of

the system to determine the receiver performance. If the noise signal level exceeds the echo signal level or very close to each other the receiver maybe unavailable to detect the beat frequency signal. Signal to noise ratio (SNR) is the ratio of the signal power to the noise power. SNR is equal to echo signal power in dBm minus the noise power in dBm. For the receiver side of the radar, thermal noise power which is the dominant noise in the system is calculated for various ports and given in Table (4.2). Using the calculated values of the thermal noise and received echo signal power in Table (4.1) the SNR of the system for various ports are given in Table (4.3).

Table 4.3 SNR Values at various ports of the receiver

d / Port	100 m.			500 m.			1000 m.		
	Signal (dBm)	Noise (dBm)	SNR	Signal (dBm)	Noise (dBm)	SNR	Signal (dBm)	Noise (dBm)	SNR
Antenna	-48.8	-96.7	47.9	-62.8	-96.7	33.9	-68.9	-96.7	27.8
Mixer Input	-36.7	-79.2	42.5	-50.7	-79.2	28.5	-56.8	-79.2	22.4
Mixer Output	-44.2	-114.4	70.2	-58.2	-114	56.2	-64.3	-114	50.1
DSP Input	24.6	-44.7	69.3	10.6	-44.7	55.3	4.5	-44.7	49.2

Signal to noise ratios of the system at various ports are fairly large enough for radar to function properly within the maximum range of 1000 meters.

4.5 Component Tests

Throughout this section the results of the component test for some components are given. Tests are conducted for some important variables and the results are compared with the manufacturers' specifications. VCO, low pass and band pass filters and switch are tested and some measurements are done for critical specifications of each component.

The performance of the complete radar system will be done by using delay elements which are able to add a time delay to the transmitted signal, this time delay corresponds to a fixed target distance. Component tests for fixed delay line are also conducted and the results are given as well.

Evaluation boards are fabricated using Roger-4003 substrate with a relative dielectric constant of 3.4. Thickness of the substrate is 0.51 mm. The line width with characteristic impedance of Z_c=50Ω was calculated using microwave design program CNL.

The input and output return losses are obtained from S_{11} and S_{22} parameters respectively. S_{12} is the reverse isolation that is the signal that gets from output port to the input. Gain of the network obtained from the S_{21} parameter. S-parameters measurements were performed with a HP-8720D Network Analyzer. Frequency spectrum was measured using a HP-70004A Spectrum Analyzer. A HP-83640A Synthesized Sweeper was used as the local oscillator.

4.5.1 Voltage Controlled Oscillator (VCO)

Frequency deviation (ΔF) of the pulse FMCW radar can be achieved by using suitable VCO. Applying continuously changing tuning voltage to the VCO will result a triangular frequency modulation. VCO of the Mini-Circuits, JTOS-1025 Figure (4.14), was tested. Specifications of Mini-Circuits for JTOS-1025 are given in Table (4.4).

Table 4.4 JTOS-1025 Specifications

Frequency (MHz)		Power Output (dBm)	Tuning Sensitivity (MHz/V)	Harmonics (dBc)		Power Supply	
Min	Max	Typical	Typical	Min	Max	Voltage (V)	Current (mA)
685	1025	8.6	21-36	-28	-20	12	22

Figure 4.14 Photograph of JTOS-1025

JTOS-1025 was operated by a voltage supply and results were observed using Frequency Spectrum. The results are given in Table (4.5).

Table 4.5 JTOS-1025 Test results

Tuning Voltage (V)	Frequency (MHz)	Power Output (dBm)	Harmonics (dBc)		Power Supply	
			Second	Third	Voltage (V)	Current (mA)
7.76	848.75	9.6	-	-	12	19
7.8	850	9.6	-	-	12	19
8.5	875	9.8	-	-	12	19
9.2	900	9.9	-	-	12	19
13.2	1020	10.2	-24.2	-50.2	12	19

Results show that JTOS-1025 has very similar specifications with the manufacturers. Tuning sensitivity within 850 and 1000 MHz was 31 MHz/V. The measured output power was greater than the expected value. A second harmonic of the center frequency 1020 MHz was measured 24.2 dB less than the fundamental. A third harmonic with a power level

50.2 dB less than the fundamental was measured at 3060 MHz. These harmonics will be suppressed approximately 50 dB by using a low pass filter at the output of the VCO. No spurious signal was observed.

4.5.2 Low Pass Filter (LPF)

Low pass filter will be used for suppression of the harmonics from the VCO. Two different low pass filters was measured. Both have the cut-off frequency of 1000 MHz. SCLF-1000 from Mini-Circuits and LMS1000-5CC from Lark Engineering was measured. Photograph of both filters is given in Figure (4.15).

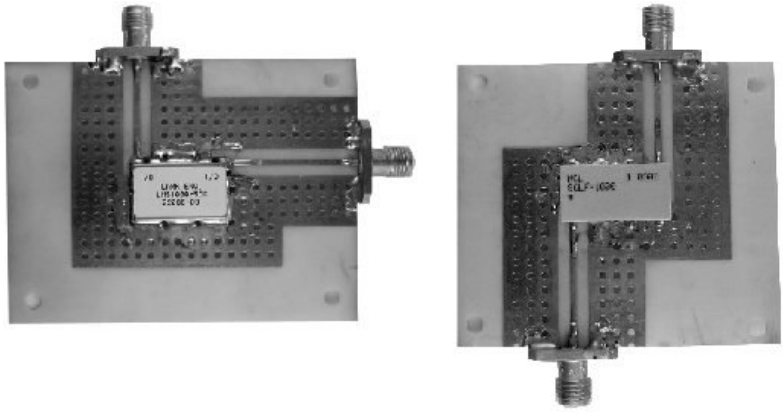

Figure 4.15 Photograph of SCLF-1000 (left) and LMS1000-5CC (rigth)

Pass band is very clear for both filters below 1 GHz that is the cut-off frequency. The attenuation at the first stop band is very high. The specifications of both filters are suitable for the harmonic suppression. Frequency response of SCLF-1000 and LMS1000-5CC are given in Figure (4.16). The characteristic of LMS1000-5CC is much more ideal than the characteristics of SCLF-1000.

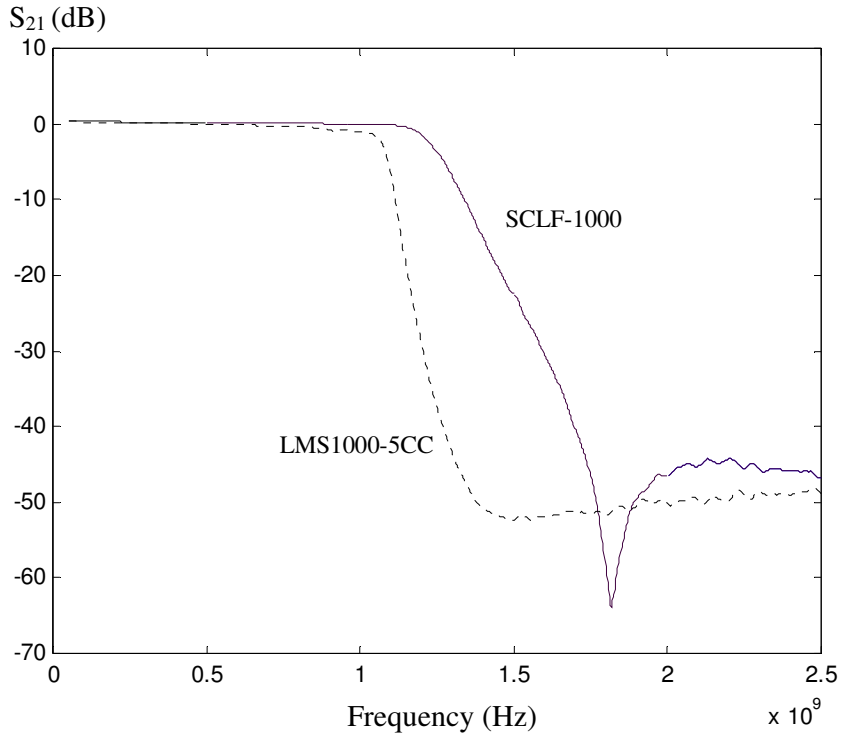

Figure 4.16 Frequency response of SCLF-1000 and LMS1000-5CC

4.5.3 Band Pass Filter (BPF)

Band pass filter in the system will be used for noise reduction, and suppression of unwanted low frequency and high frequency signals compared to the carrier signal. The carrier signal that is f_c is between 800-900 MHZ. The band pass filter center frequency is 850 MHz. MS850-161-4CC band pass filter is chosen from Lark Engineering. Photograph of the BPF given in Figure (4.17). S_{21} parameter that is the frequency response of the filter is given in Figure (4.18).

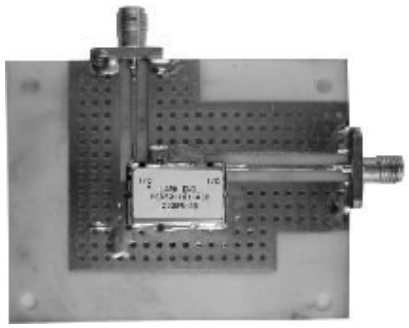

Figure 4.17 Photograph of MS850-4CC

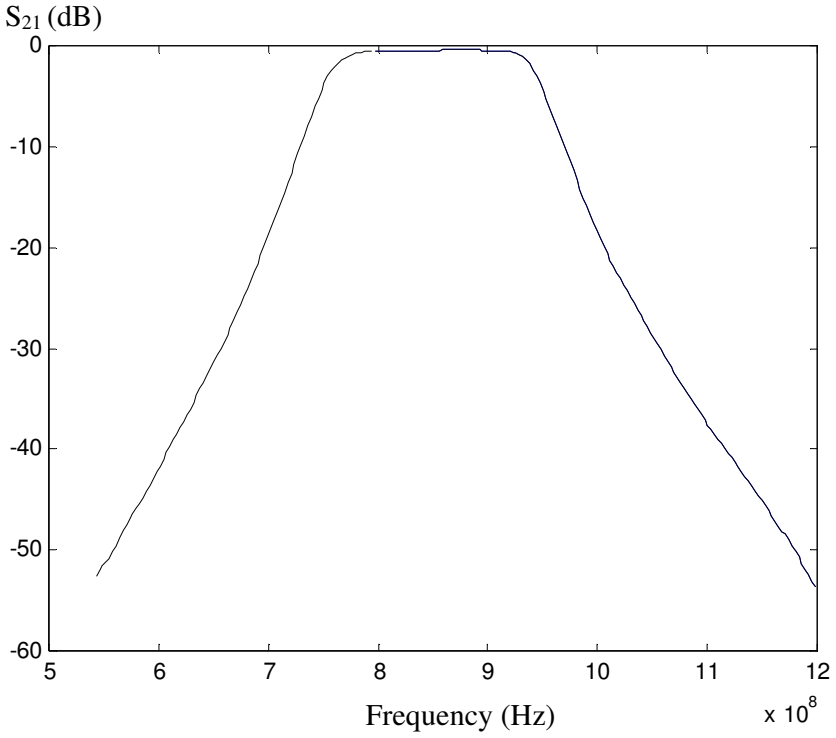

Figure 4.18 Frequency response of MS850-4CC

Band pass filter MS850-4CC has a very linear response within 800-900 MHz bandwidth. The frequency response is very suitable for pulse FMCW radar.

4.5.4 Circulator

Transmitted signal and the received echo are separated using a circulator. Circulator is a 3-port ferrite device.

From port 1 to 2 the signal pass without very low attenuation but the reverse path from port 2 to 1 the attenuation is very high. Also the ports 1 and 3 are isolated. The transmitted signal path is from port 1 to 2 and the echo signal path is from port 2 to 3. Photograph of the circulator X800L-100 of Anaren given in Figure (4.19).

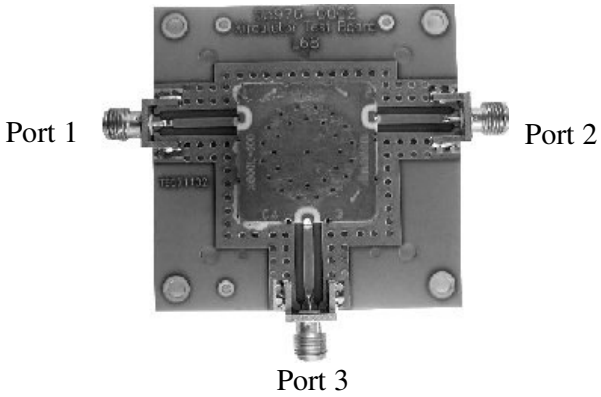

Figure 4.19 Photograph of X800L-100

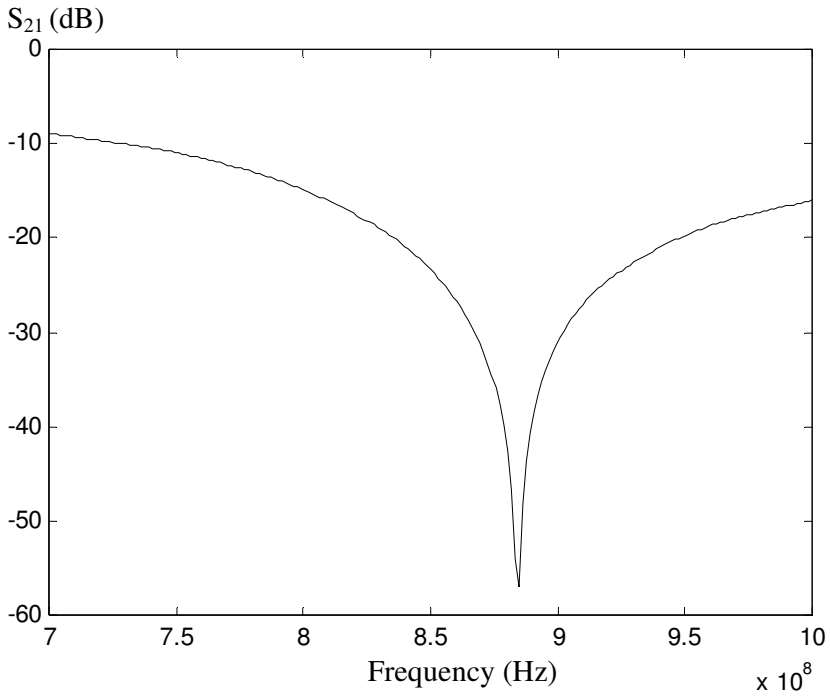

Figure 4.20 Isolation of circulator from port 1 to 3

The isolation must be as great as possible between port 1 and 3 to reduce the leaking noise from transmitter to receiver. In Figure (4.20) isolation between ports 1 and 3 is given. Insertion losses from port 1 to 2 and from port 2 to 3 are less than 1 dB. Isolation has maximum with a value of 57 dB at 885 MHz from port 1 to 3.

4.5.5 Switch

Switches are operated such to determine the transmitting and receiving modes of the radar. There are two switches operating reversely. Thus the noise from VCO cancelled when the radar is on receiving (listening) mode. The isolation of the switches when they are off is the important parameter to reduce or cancel the leakage noise from VCO. Mini-Circuits switch KSWHA-1-20 chosen, the photograph of the evaluation board of the switch given in Figure (4.21).

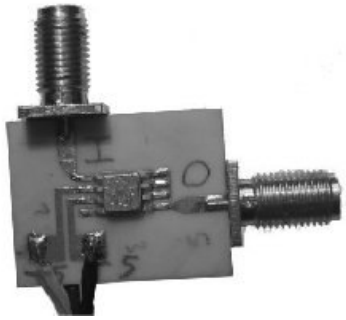

Figure 4.21 Photograph of KSWHA-1-20

Insertion loss of the switch is less than 1 dB and the isolations towards input to output and output to input are approximately 50 dB.

4.5.6 Antenna

Antenna is one of the important parts of the radar system. Antenna determines where the generated power will be transmitted in free space. The antenna used has a very large

beamwidth on both θ and Φ axes. The normalized field pattern of the antenna is given in Figure (4.4). Photograph of the mounted antenna is given in Figure (4.22).

Figure 4.22 Photograph of the antenna

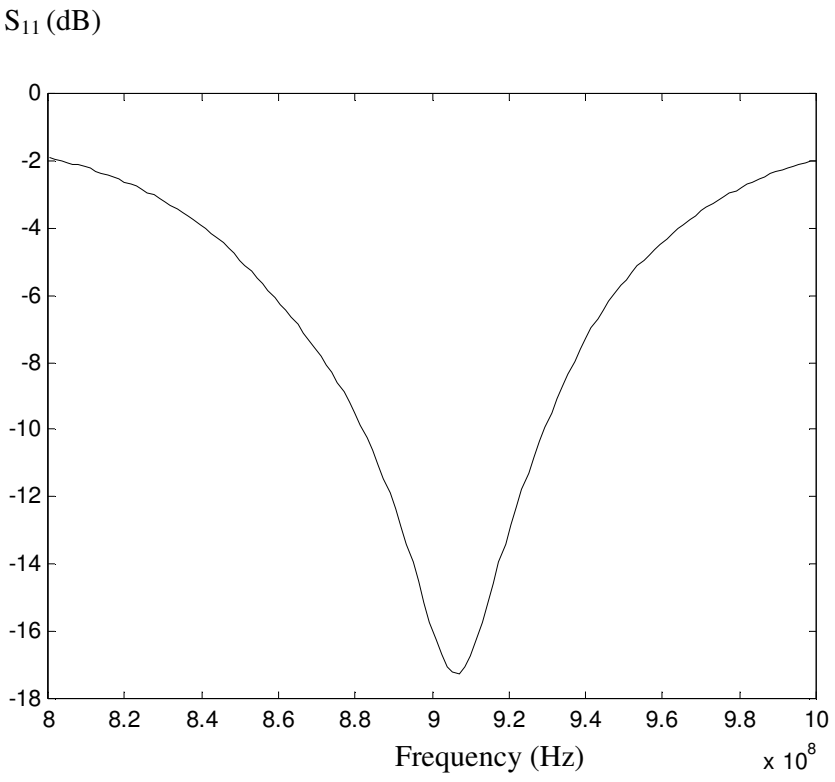

Figure 4.23 Antenna Return Loss

Mismatch of the antenna will result to loss of power thus the antenna must have a return loss (S_{11}) as large as possible.

Antenna is aligned for a center frequency of 9.06 MHz. After mounting a radome to the antenna the center frequency will be shifted to a lower level that is the operating frequency. E and H normalized directivity patterns are given in Appendix D and E respectively.

4.6 Radar Test Board

In the laboratory environment the system tests for the radar must be conducted. The range of the radar is greater than 1000 meters. To perform the tests and simulating the target suitable delay lines may be used. Using a coaxial delay line length of 1000 meters will result a very high attenuation on the transmitted signal. The transmitted signal power will decay to the noise signal levels at the end of the transmission line therefore receiving of the transmitted signal will be unavailable. Another choice is the using fiber optics for the transmission line. But there must be additional encoder and decoder circuitry for converting carrier signal to the visible light. In either coaxial line or fiber optic the length of the transmission line is 1000 meters and for different distance of the target different lengths of the transmission lines must be provided.

Another cheap and easy method of target simulation and providing delay to the transmitted signal is to use SAW filters discussed in Chapter 3. The SAW filter actually a delay line. The SAW velocity (ν_s) of $LiNbO_3$ is approximately 3500 m/s thus for a delay of 2.85 microseconds only a 1 cm length of $LiNbO_3$ substrate is sufficient. Also the practical

bandwidth for $LiNbO_3$ is very large so for higher frequency deviations (ΔF) of the radar SAW delay line can be used as well. For the center frequency of 850 MHz a SAW delay line fabricated on $LiNbO_3$ substrate can be used for frequency deviation up to 200 MHz. But for SAW delay lines fabricated on GaAs substrate the maximum frequency deviation allowed is about 25 MHz at the same center frequency.

SAW delay line SF0850DL01825T from Micro Networks chosen for a fixed delay of 2.5 microseconds. Manufacturer's specification for SAW delay line is given in Table (4.6).

Table 4.6 SAW Delay line specifications

Parameter	Min	Typical	Max	Units
Center Frequency		850		MHz
Insertion Loss		24	27	dB
3 dB Bandwidth	80	240		MHz
PB Amplitude Ripple		1.0	2.0	dB p-p
Delay	2.45	2.5	2.55	µsec
Material		YZ-$LiNbO_3$		

Insertion Loss of the delay line is typical 27 dB. Due to high insertion loss SAW delay line can be used without any additional attenuator. Photograph of the radar test board given in Figure (4.24).

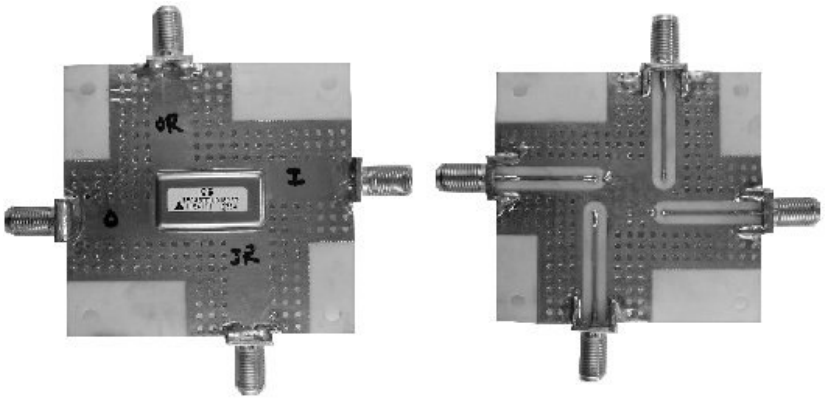

Figure 4.24 Photographs of radar test board

Test board's S-parameters and associated delay was measured. The frequency response (S_{21}) is given in Figure (4.25) and the phase response given in Figure (4.26).

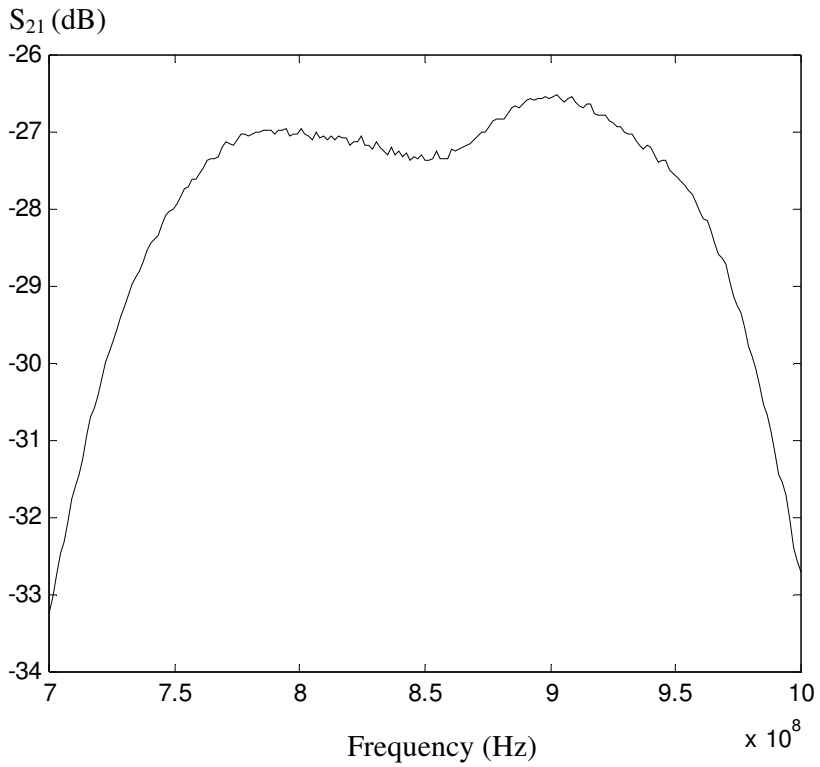

Figure 4.25 Test board frequency response

Insertion loss of the test board varies between −26.5 to −27.5 dB. Center frequency is 850 MHz and the 3 dB bandwidth is equal to 250 MHz. Delay of the test board calculated from the phase of the system.

If we add a delay to the reference signal as long as the delay of the test board phase of the system will be calculated as zero. To determine this delay marker→delay method of the network analyzer HP 8720D was used. Network analyzer was automatically calculated the electrical length and the associated delay of the network. Measured electrical

delay and associated electrical length and simulated target distance given in Table (4.7).

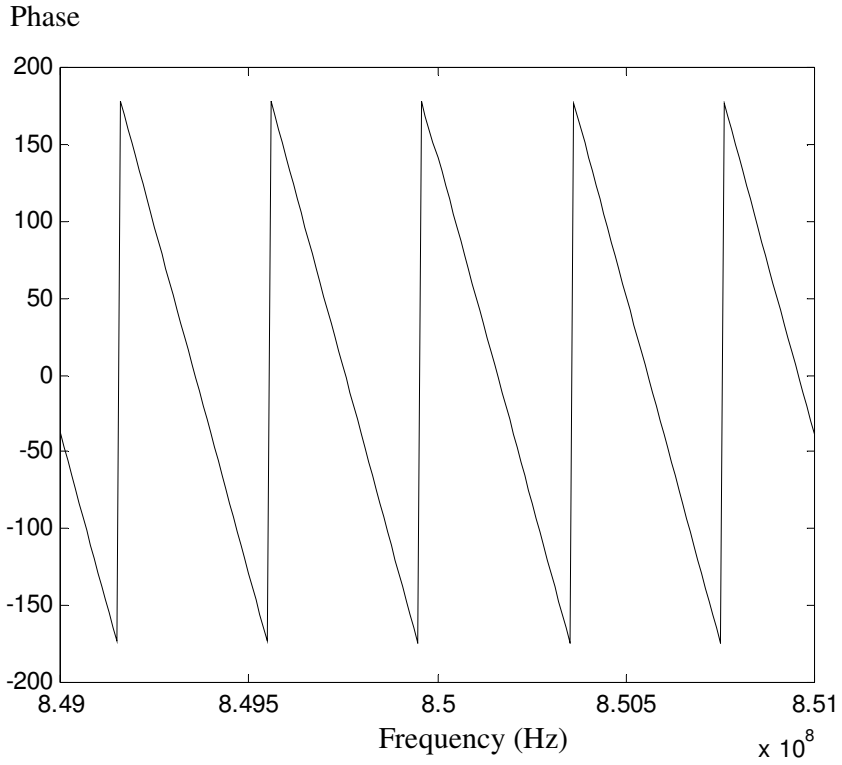

Figure 4.26 Phase of the test board

Table 4.7 Delay of the test board

Frequency (MHz)	Delay (μsec)	Electrical Length (m)	Simulated Target Distance (m)
800	2.48	743.5	371.7
850	2.49	746.5	373.2
900	2.51	752.5	376.2

Two delay lines cascaded will result a delay of approximately 5 µsec. The insertion loss of the two delay line system is given in Figure (4.27).

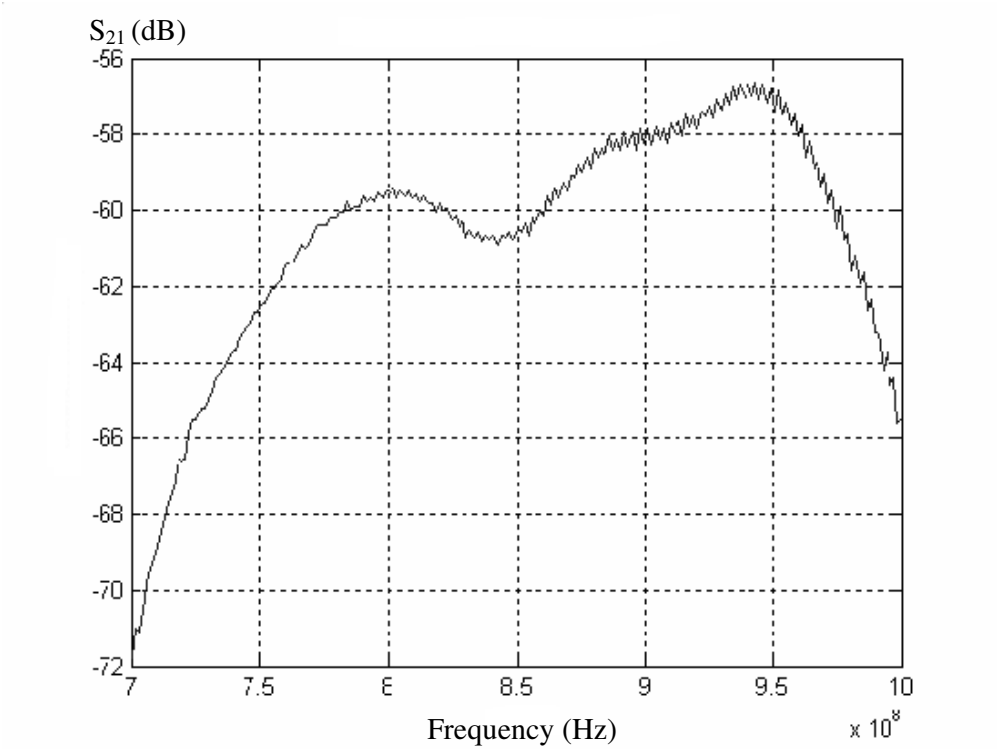

Figure 4.27 Insertion loss of cascaded two delay lines

Total delay associated the two delay lines was measured by marker→delay method of the network analyzer as 5.0035 µsec. This time delay corresponds to a distance of 749.5 meters.

4.7 Alternative Test Method

Test board with SAW delay line focused on adding a suitable time delay to the reference signal. Radar determines the distance to target by measuring the beat frequency corresponding to time delay. Time delay results a shift between the reference signal and transmitted signal this frequency difference is the beat frequency. Instead of delaying the transmitted signal a beat frequency injection to the transmitted signal at the transmission time (t=0)

will also result a beat frequency in the IF side of the radar receiver.

In the alternative method we add an artificial time delay by adding a beat frequency to the carrier signal. Schematic view of the alternative test board is given in Figure (4.27).

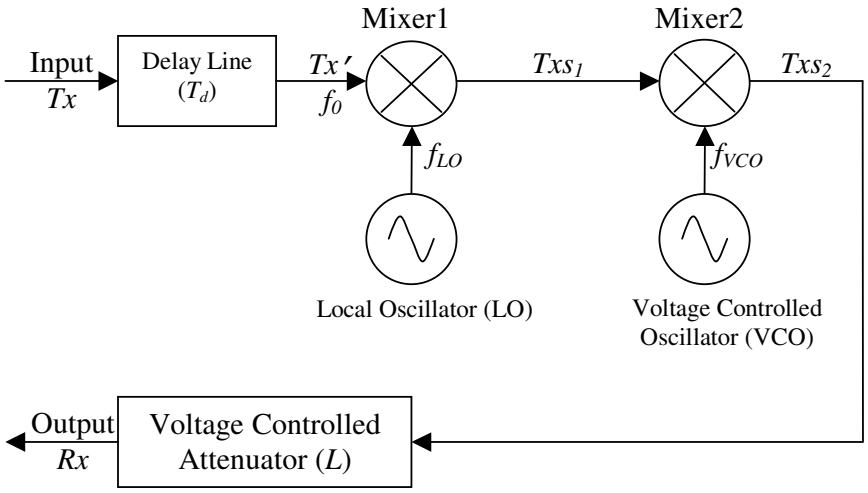

Figure 4.28 Alternative test board

If the transmitted signal is *Tx*, delayed signal is *Tx′*, shifted signals at the output of the mixer1 and mixer2 are Txs_1 and Txs_2 and the signal send back to the radar is *Rx* and *k* is being the mixer constant then;

$$Tx = A\,Cos(\omega_0 t + \phi) \tag{4.49}$$

$$Tx' = A\,Cos(\omega_0 t' + \phi), \qquad t' = t + T_d \tag{4.50}$$

$$V_{LO} = B\,Cos(\omega_{LO} t' + \phi_{LO}) \tag{4.51}$$

$$V_{VCO} = C\,Cos(\omega_{VCO}t' + \phi_{VCO}) \tag{4.52}$$

$$Txs_1 = A\,Cos(\omega_0 t' + \phi) \times BCos(\omega_{L0}t' + \phi_{LO}) \times k \tag{4.53}$$

$$Txs_2 = ACos(\omega_0 t' + \phi) \times BCos(\omega_{L0}t' + \phi_{LO}) \times CCos(\omega_{VCO}t' + \phi_{VCO}) \times k^2 \tag{4.54}$$

Thus final signal *Rx* which is send back to the radar with a suitable attenuation (*L*) is equal to Equation (4.55).

$$\begin{aligned} R_x = K \times \{ & Cos[(\omega_0 + \omega_{LO} + \omega_{VCO})t' + \phi + \phi_{LO} + \phi_{VCO}] \\ & + Cos[(\omega_0 + \omega_{LO} - \omega_{VCO})t' + \phi + \phi_{LO} - \phi_{VCO}] \\ & + Cos[(\omega_0 - \omega_{LO} + \omega_{VCO})t' + \phi - \phi_{LO} + \phi_{VCO}] \\ & + Cos[(\omega_0 - \omega_{LO} - \omega_{VCO})t' + \phi - \phi_{LO} - \phi_{VCO}]\} \end{aligned} \tag{4.55}$$

where

$$K = \frac{L \times A \times B \times C \times k^2}{4} \tag{4.56}$$

In the radar *Rx* is the received signal which will proceed through the RF port of the mixer shown in Figure (4.9). The signal at the LO port of the mixer (V_{LO}') is

$$V_{LO}{}' = A'\,Cos(\omega_0' t' + \phi) \tag{4.57}$$

The signal at the IF port of the mixer (V_{IF}) in the radar can be expressed by equation (4.58).

$$\begin{aligned} V_{IF} = \zeta_1 \times \{ & Cos[(\omega_0 + \omega_0' + \omega_{LO} + \omega_{VCO})t' + 2\phi + \phi_{LO} + \phi_{VCO}] \\ & + Cos[(\omega_0 + \omega_0' + \omega_{LO} - \omega_{VCO})t' + 2\phi + \phi_{LO} - \phi_{VCO}] \\ & + Cos[(\omega_0 + \omega_0' - \omega_{LO} + \omega_{VCO})t' + 2\phi - \phi_{LO} + \phi_{VCO}] \\ & + Cos[(\omega_0 + \omega_0' - \omega_{LO} - \omega_{VCO})t' + 2\phi - \phi_{LO} - \phi_{VCO}] \\ & + Cos[(\omega_0 - \omega_0' + \omega_{LO} + \omega_{VCO})t' + \phi_{LO} + \phi_{VCO}] \\ & + Cos[(\omega_0 - \omega_0' + \omega_{LO} - \omega_{VCO})t' + \phi_{LO} - \phi_{VCO}] \\ & + Cos[(\omega_0 - \omega_0' - \omega_{LO} + \omega_{VCO})t' - \phi_{LO} + \phi_{VCO}] \\ & + Cos[(\omega_0 - \omega_0' - \omega_{LO} - \omega_{VCO})t' - \phi_{LO} - \phi_{VCO}]\} \end{aligned} \tag{4.58}$$

$$\zeta_1 \approx 0.087 \times A \times B \times C \times L \times k^2 \tag{4.59}$$

IF signal at the receiver side of the radar is filtered by the beat frequency filters. Beat frequency filter is a series of low pass (f_{cutoff}=10 KHz) and high pass filter (f_{cutoff}=150 KHz). We adjust ω_{LO}-ω_{VCO} to be the desired beat angular frequency for example; f_{LO}=10 MHz and f_{VCO}=9.9 MHz for a beat frequency for a beat frequency of 100 KHz. After the filtering the IF signal V_{IF} the resultant signal at the input port of the digital signal processor V_{DSP} is:

$$\begin{aligned} V_{DSP} = \zeta_2 \times \{ & Cos[(\omega_0 - \omega_0' + \omega_{LO} - \omega_{VCO})t' + \phi_{LO} - \phi_{VCO}] \\ & + Cos[(\omega_0 - \omega_0' - \omega_{LO} + \omega_{VCO})t' - \phi_{LO} + \phi_{VCO}]\} \end{aligned} \tag{4.60}$$

where

$$|\omega_{LO} - \omega_{VCO}| = \omega_{beat} = 2\pi f_b \tag{4.61}$$

$$\omega_0 - \omega_0' = 2\pi(3750) \tag{4.62}$$

$$\zeta_2 \approx 10^7 \times L \times A \times B \times C \times k^2 \tag{4.63}$$

then V_{DSP} can be expressed by Equation (4.64).

$$\begin{aligned} V_{DSP} = \zeta_2 \times \{ & Cos[2\pi(f_b - 3750)t' + \phi_{LO} - \phi_{VCO}] \\ & + Cos[2\pi(f_b + 3750)t' + \phi_{LO} - \phi_{VCO}]\} \end{aligned} \tag{4.64}$$

Delay line used in the alternative test method has a delay (T_d) corresponding to an electrical length of minimum 30 meters. This delay must be greater than 100 nanoseconds which is the pulse duration of the transmitted signal. When the pulse radar is in transmission mode which lasts for 100 nanoseconds the receiver switch is on open position. Thus

for receiver switch to close we must wait for minimum 100 nanoseconds which is the pulse duration.

Theoretically one mixer is enough for artificial time delay generation. However there is a limit for the frequency of the LO port of many traditional mixers. For the chosen mixer which IF port handles up to 1 GHz frequency input and the LO port input signal frequency must be greater than 5 MHz. This limitation is handled by using two mixers consecutively and adjusting the local oscillator and voltage controlled oscillator frequencies to be greater than 5 MHz. The mixer MD54-0004 from M/A Com for mixer1 and mixer2 and programmable waveform generator AD9833 from analog devices for local oscillator and voltage controlled oscillator are suitable for implementation.

CHAPTER 5

CONCLUSION

A pulse FMCW radar design investigated in detail. The transmitted and received echo signal power levels calculated and noise of the system determined. With the presence of noise SNR values for various ports of the receiver calculated. For the chosen frequency resolution (Δf_b = 1.172 KHz) the noise levels remain very low from the received signal power level. Thus the radar performance within the range of 1000 meters found to be very effective. The noise level is directly proportional to the bandwidth of the signal thus increasing the frequency resolution yields an increase in the noise power.

Essential specifications of some components was measured and found to be suitable for the implementation of the pulse FMCW radar.

A very simple test board with high insertion loss using surface acoustic wave (SAW) filter implemented. High insertion loss corresponds to the free space and reflection losses. Free space losses are greater than the insertion loss of the test board. In addition to the test board insertion loss simple coaxial attenuators of 22 dB and 44 dB may also be used to increase the attenuation as well. Using one SAW delay line (filter) a delay corresponding to approximately 370 meters was simulated in the laboratory environment. Two series of the test board will yield a total delay of 740 meters with the total insertion loss of 55 dB and three in series yield to a total delay corresponding to

1110 meters with a attenuation of 84 dB. Radar test board utilizes only fixed delays of 370, 740 and 110 meters. To achieve a variable delay from 100 meters up to 1000 meters for completely simulating target an artificial time delay generation method presented as well. Artificial delay acquired by adding a beat frequency the carrier signal instantaneously instead of delaying the carrier. In the alternative method a variable voltage source varies the injected beat frequency.

REFERENCES

[1] M. I. Skolnik, "Introduction To Radar Systems", McGraw-Hill Int. Book Co., 1983.

[2] URL: http://www.mtt.org

[3] A. Hızal, EE-625 Lecture Notes, Middle East Technical University, Ankara, 2001.

[4] C. A. Balanis, "Antenna Theory", John Wiley & Sons, Inc., 1997.

[5] O. G. Villard, "Radio Science", vol.11, 1976.

[6] M. Feldmann and J. Hénaff, "Surface Acoustic Waves For Signal Processing", Artect House, 1989.

[7] C. F. Brockelsby, "Ultrasonic Delay Lines", Iliffe Books Ltd, 1963.

[8] V. M. Ristic, "Principles of Acoustic Devices", John Wiley & Sons, Inc., 1983.

[9] K. Hashimoto, "Surface Acoustic Wave Devices in Telecommunications: Modeling and Simulation", Springer-Verlag, 2000.

[10] F. E. Nathanson, "Radar Design Principles", 2 nd Edition, Mc Graw Hill, Inc., 1990.

[11] Mini-Circuits, "VCO/HB-01 VCO Designer's Handbook 2001", Mini-Circuits Division of Scientific Components, NY, 2001.

APPENDIX A

RADAR FREQUENCIES

Table A.1 Radar Frequencies

Band Designation	Nominal Frequency Range	Specific Radiolocation Radar Bands ITU Assignments
HF	3–30 MHz	
VHF	30–300 MHz	118–144 MHz 216–225 MHz
UHF	300–1000 MHz	420–450 MHz 890–942 MHz
L	1–2 GHz	1215–1400 MHz
S	2–4 GHz	2.3–2.5 GHz 2.7–3.7 GHz
C	4–8 GHz	5.25–5.925 GHz
X	8–12 GHz	8.5–10.68 GHz
K_u	12–18 GHz	13.4–14.0 GHz 15.7–17.7 GHz
K	18–27 GHz	24.05–24.25 GHz
K_a	27–40 GHz	33.4–36.0 GHz
mm	40–300 GHz	

APPENDIX B

DOPPLER FREQUENCY AS A FUNCTION OF OSCILLATION FREQUENCY AND SOME RELATIVE TARGET VELOCITIES

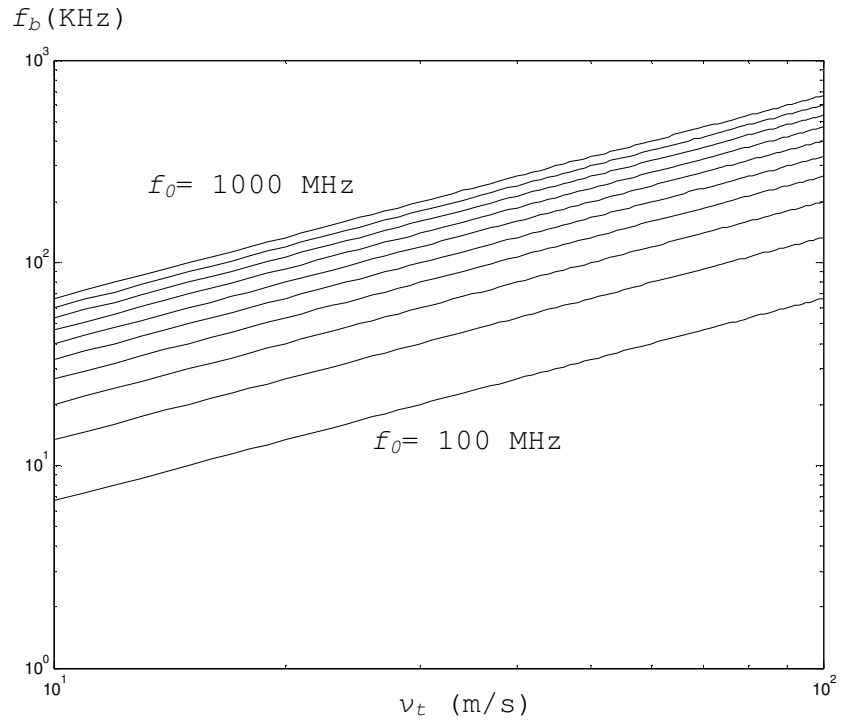

Figure B.1 Doppler frequency versus target velocity (*fo*=100,200,…,900,1000 MHz)

APPENDIX C

MATLAB 6.5 M-Files

1.) directPr.m:

```
%directPr.m calculates Pr directly for θ where θ is evaluated as constant.
clear
Teta1=input ('Teta=');
Teta=abs(Teta1);
f=input('Center frequency (MHz)=');
d=input('Distance (m)=');
TetaB=80;
c=3*10^8;
lambda=c*10^-6/f;
Y=((10.^(-0.15.*2.^1.5.*(abs(Teta-
30)/TetaB).^1.5).^4).*cos(Teta*pi/180).^2).*10.^
(-1.4.*(1-exp(-(0.2.*Teta))));
Q=1000*6.3^2*lambda^2*(pi/180)^2*80/((4*pi)^3*d^2);
Pr=10*log10(Y*Q);
plot(Teta1,Pr,'k');
disp(Q);
```

2.) Pr.m:

```
%Pr.m calculates Pr evaluating integral from θ to θ+θΔ.
clear
k=1;
Teta0=0;
Teta1=input ('Teta=');
f=input('Center frequency (MHz)=');
d=input('Distance (m)=');
DelTeta=input('Δθ=');
lambda=3*10^2/f;
```

```
Q=1000*6.3^2*lambda^2*(pi/180)^2*80/((4*pi)^3*d^2)
count=0;
for i=1:length(Teta1);
    count=count+1;
    Teta=abs(Teta1(count));
    YQ=10.*log10(quad(@prfun,Teta,Teta+DelTeta).*Q);
    PR(k)=YQ;
    k=k+1;
end;
plot(Teta1,PR,'k')
disp(Q)
```

3.) prfun.m:

```
%prfun.m is used to identify the function which will be
evaluated by Pr.m and beatvariation.m
function Y=prfun(Teta);
Teta0=30;
TetaB=80;
Y=((10.^(-0.15.*2.^1.5.*(abs(Teta-
Teta0)/TetaB).^1.5).^4).*cos(Teta*pi/180).^2).*10.^(-
1.4.*(1-exp(-(0.2.*Teta))));
```

4.) beatvariation.m:

```
% beatvariation.m calculates the received echo (Pr) for a
given Δfb
clear
f=input('Center frequency (MHz)=');
d=input('Distance (m)=');
c=3*10^8;
dfb=input('Delta fb (KHz)=')*10^3;
lambda=c*10^-6/f;
fb=input('fb limits (Hz)=');
K=125;
```

```
Q=1000*6.3^2*lambda^2*(pi/180)^2*80/((4*pi)^3*d^2);
count=1;
for i=1:length(fb)
   fb1=fb(i);
   Teta1=real(acos(K*d/(fb1-dfb/2)))*180/pi;
   Teta2=real(acos(K*d/(fb1+dfb/2)))*180/pi;
   YQ=10.*log10(quad(@prfun,Teta1,Teta2).*Q);
   PR(count)=YQ;
   count=count+1;
end
plot(fb,PR,'k');
disp(Q);
disp(K);
```

APPENDIX D

E-Plane Normalized Directivity Pattern (θ=0°)

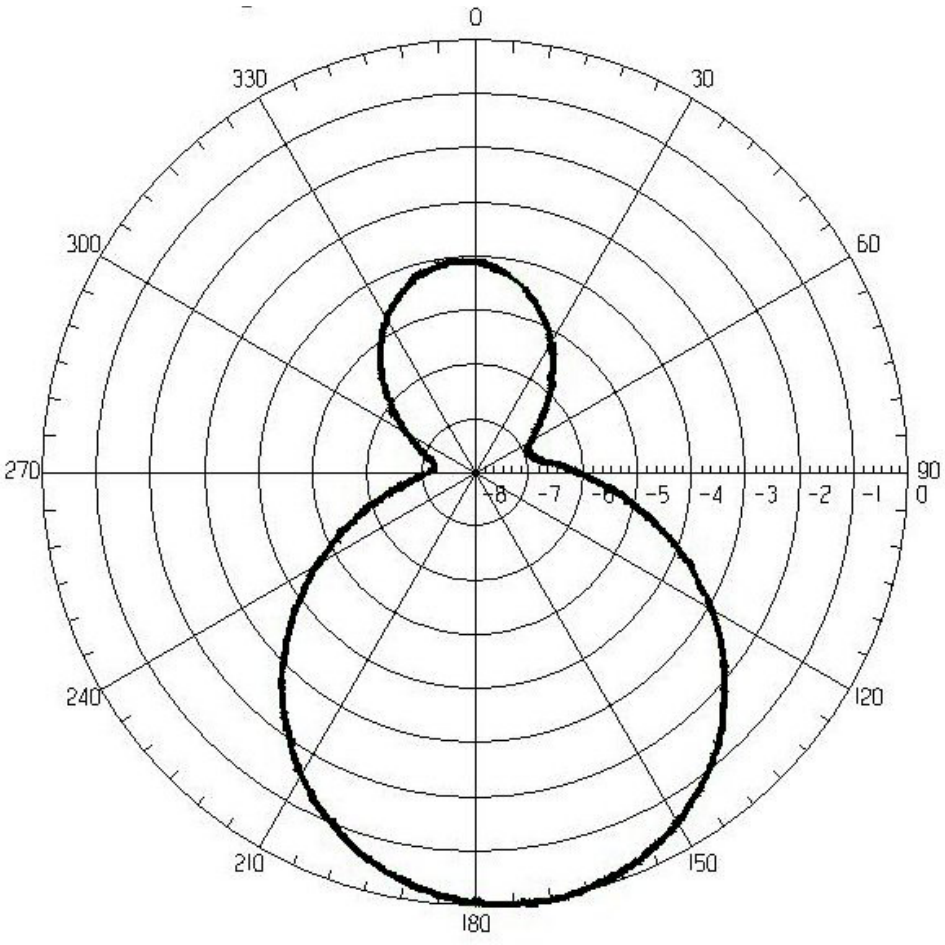

Figure D.1 E-Plane normalized directivity pattern

APPENDIX E

H-Plane Normalized Directivity Pattern (θ=-90°)

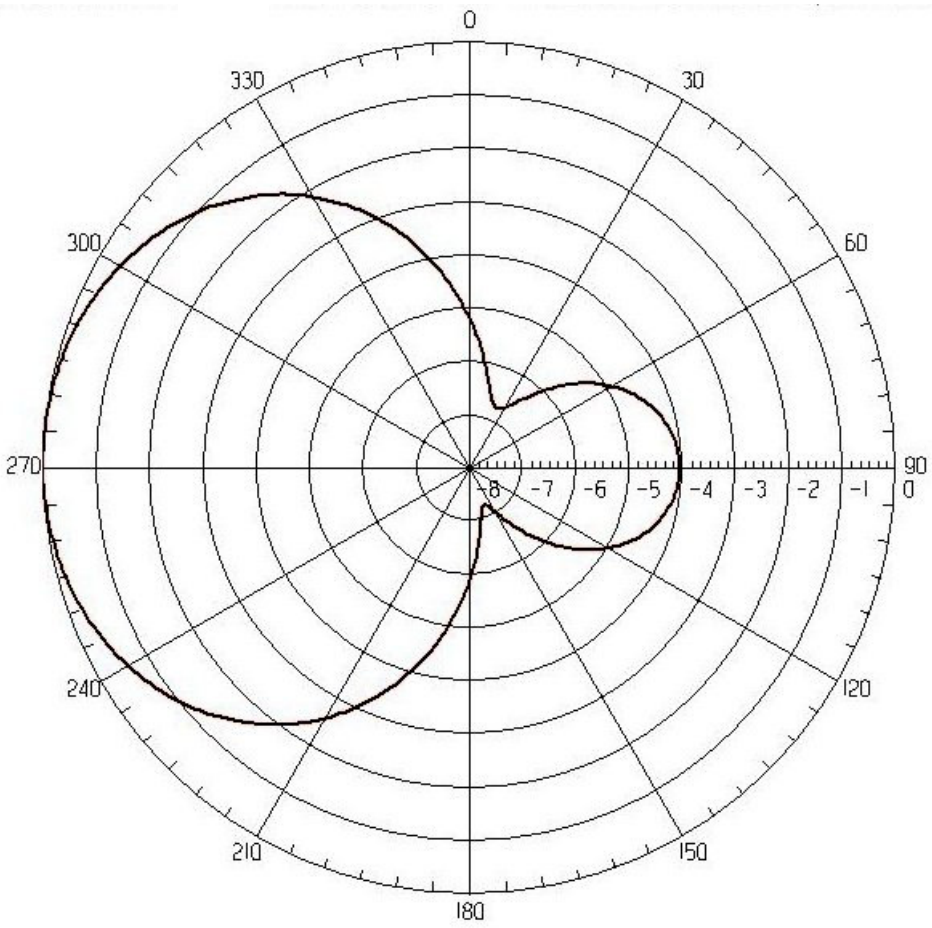

Figure E.1 H-Plane normalized directivity pattern